THE ASTROPHYSICAL JOURNAL, 446:646–664, 1995 June 20

STUDIES OF HOT B SUBDWARFS. X. THE DISTRIBUTION AND SPACE DENSITY OF HOT, HYDROGEN-RICH SUBDWARFS DETERMINED FROM THE PALOMAR-GREEN SURVEY[1]

B. VILLENEUVE,[2] F. WESEMAEL, G. FONTAINE, AND C. CARIGNAN
Département de Physique, Université de Montréal, C.P. 6128, Succ. Centre Ville, Montréal, Québec, Canada H3C 3J7;
villeneu, wesemael, fontaine, claude@astro.umontreal.ca

AND

R. F. GREEN
Kitt Peak National Observatory, National Optical Astronomy Observatories, P.O. Box 26732, Tucson, AZ 85726-6732; rgreen@noao.edu
Received 1994 November 9; accepted 1994 December 22

ABSTRACT

We have computed the space density, as well as the characteristic scale height of the distribution, of hot, hydrogen-rich subdwarfs in the Galaxy through the use of photoelectric Strömgren photometry of a sample of 209 of these stars culled from the Palomar-Green Survey. Homogeneous, exponential, and isothermal-sheet model distributions in the direction perpendicular to the Galactic plane are considered in turn, together with various subsamples of objects reaching down to different limiting b magnitudes. Taking into account the results of the V/V_m test on the brightest subsamples, which suggest that the PG survey might not be complete at bright magnitudes, we find that the distribution of hot, hydrogen-rich subdwarf stars can be satisfactorily reproduced with an isothermal scale height of 600 ± 150 pc, a value characteristic of the disk population of spiral galaxies or, alternatively, with an exponential scale height of 450 ± 150 pc. The resulting values of the space density and birthrate in both cases are $(3 \pm 1) \times 10^{-7}$ pc^{-3} and $\sim(1\text{–}3) \times 10^{-15}$ pc^{-3} yr^{-1}, a factor of $\sim$5–10 lower than previous estimates. Detailed comparisons with previous determinations are provided, and the implications of the large exponential scale height, and low space density and birthrate, for this particular channel of pre–white dwarf evolution are considered.

Subject headings: Galaxy: structure — stars: early-type — stars: statistics — subdwarfs

1. INTRODUCTION

Twenty years after the pioneering work of Greenstein & Sargent (1974) on the nature of faint, subluminous stars at high Galactic latitudes, our knowledge of hot, hydrogen-rich subdwarf (sdB and sdOB) stars has flourished. Systematic colorimetric searches for faint blue stars, combined with detailed model atmosphere analyses of increasingly larger samples of such stars, now yield a fairly complete picture of the physical properties and evolutionary status of the hydrogen-rich subdwarfs. The reviews of Heber (1987, 1991) summarize our current knowledge of these objects on several fronts.

One of the significant advantages of working with the large-scale, colorimetric surveys of faint blue stars, like the Palomar-Green (PG; Green, Schmidt, & Liebert 1986) and the Kitt Peak–Downes (KPD; Downes 1986) surveys, is the fact that hot subdwarfs dominate the population of stellar objects down to $B \sim 16.5$. These surveys thus yield large, homogeneous samples of hot subdwarfs, which are amenable to statistical analyses. One of the primary aims of such analyses should be to get a reliable estimate of the space density of hot, hydrogen-rich subdwarfs, as well as an accurate description of the properties of their distribution in the Galaxy. This, in turn, would help us define what fraction of white dwarf stars evolve from hot subdwarfs rather than from planetary nebula nuclei. It would, as well, help us confirm whether their distribution is characteristic of a disk, albeit an old disk, population—as is currently thought—and would permit a comparison of the scale heights of hot, hydrogen-rich subdwarfs with those of the helium-rich sdO stars, of the white dwarfs, and of planetary nebula nuclei.

These problems have been addressed in the past. The evidence for membership of the hot, hydrogen-rich subdwarfs to an old disk population hinges, in great part, on the Baschek & Norris (1975) kinematic analysis of a sample of 17 such objects (see also the more recent preliminary results of Colin et al. 1994). These stars had previously been considered to be halo objects (Baschek & Norris 1970; Baschek, Sargent, & Searle 1972; Newell 1973; Greenstein & Sargent 1974), but an old disk population is clearly more consistent with the recent scale-height determinations of Heber (1986; 190 pc), of Green et al. (1986; 325 ± 25 pc, obtained by requiring a match to the Downes 1986 Galactic plane density), of Moehler, Heber, & de Boer (1990a; 250 pc), and of Theissen et al. (1993; 180^{+190}_{-60} pc), as well as with the kinematics of the samples studied by Saffer (1991) and Beers et al. (1992). Similarly, there seems to be agreement in these investigations, as well as in those of Reid et al. (1988) and Bixler, Bowyer, & Laget (1991), that the space density of hot, hydrogen-rich subdwarfs is in the range $(1\text{–}4) \times 10^{-6}$ pc^{-3}, a value which, once coupled to the long nuclear evolutionary times ($\tau \sim 1.5 \times 10^8$ yr) representative of extended horizontal-branch stars, suggests a fairly low birthrate for these objects ($\chi_{\rm sdB} < 3 \times 10^{-14}$ pc^{-3} yr^{-1}).

In the present paper we reconsider the problem of determining the scale height of the distribution, and the space density of hot, hydrogen-rich subdwarfs, with a large sample of such stars extracted from the PG survey. As a first step in this analysis, we have obtained photoelectric Strömgren photometry for this

[1] Based on observations obtained at the Kitt Peak National Observatory, National Optical Astronomy Observatories, which is operated by the Association of Universities for Research in Astronomy under contract with the National Science Foundation.

[2] Permanent address: Collège André Grasset, 1001 Crémazie Est, Montréal, Québec, Canada H2M 1M3.

sample of objects, and these results have already been presented in a separate paper (Wesemael et al. 1992, hereafter Paper I). In the present paper, these data are first analyzed to derive (approximate) atmospheric parameters for over 200 stars, and are then used to derive both space density and characteristic height of the distribution in the Galaxy of the hot, hydrogen-rich subdwarfs. A brief summary of the results of this analysis was presented by Villeneuve et al. (1992).

2. THE SAMPLE OF HYDROGEN-RICH SUBDWARFS

2.1. *The Color-selected PG Sample*

The Palomar-Green (Green et al. 1986) colorimetric survey covers 10,714 deg^2 divided into 266 fields. The mean completeness limit is $B_{pg} \sim 16.2$. Of the 1715 blue objects identified in the complete statistical sample, 684 are assigned internal classifications which suggest that they are hydrogen-rich hot subdwarfs. In order to make full use of that database for statistical studies of the properties of hot, hydrogen-rich subdwarfs, Wesemael et al. (1992) have obtained Strömgren photometry for 286 subdwarf candidates brighter than $B_{pg} \sim 14.6$ and selected from the *sdB*, *sdB-O*, *sd*, *sdOA*, and *sdOB* internal classes.[3] To that sample of PG subdwarfs, we added, for this study, 13 PG subdwarfs which had already been observed by Bergeron et al. (1984) but which were not reobserved in Paper I.

2.2. *Reclassifications in the PG Sample and the Problem of Completeness*

Many of the stars which may not be legitimate hydrogen-rich subdwarfs in this initial sample of 299 objects can be discarded on the basis of the morphological analysis of photometric diagrams performed in Paper I. Typical interlopers, which were not distinguished in the low-dispersion classification work of Green et al. (1986), are main-sequence late B and A stars, horizontal-branch stars, and helium-rich subdwarfs. In addition, both Moehler et al. (1990b) and Saffer et al. (1994) have obtained spectroscopic observations of many subdwarfs in the PG survey. Their spectroscopic work can be used to guide and confirm the process of photometric cleansing of the initial sample. The color criteria used for this process are discussed in Paper I. Altogether, we have removed 76 objects from our sample: 25 presumed helium-rich stars (the He-sdO class of Moehler et al. 1990b); 44 presumed low-gravity horizontal-branch or main-sequence B stars; six peculiar red objects [at $(b - y) \gtrsim +0.250$], and one confirmed white dwarf star. We are left, for now, with a sample of 223 objects.

In parallel, we need to evaluate the number of hydrogen-rich subdwarfs which might have been *missed* through misclassification by Green et al. The most likely possibility is that some hydrogen-rich subdwarfs have been classified as DA stars in the course of the survey. Fortunately, the DA sample of the PG catalog has by now been rather thoroughly investigated by Fleming, Liebert, & Green (1986) and by Bergeron, Saffer, & Liebert (1992). The former report that about half of the DA white dwarf sample used by Green (1980) for his initial determination of the space density of white dwarfs were later reclassified as "lower gravity" objects (i.e., hot subdwarfs). These reclassifications are included in the published catalog of Green et al., and are thus accounted for in our photometric sample. More recently, Bergeron et al. (1992) have reclassified an additional 10 "DA white dwarfs" of the PG survey as lower gravity objects. However, only one of these objects, the "DA 2 white dwarf" PG 1430+427, is sufficiently bright ($B_{pg} = 14.55$, $V = 14.47$) that it *would have been* included in our photometric survey had it been classified properly in the PG catalog. There are no published Strömgren colors for this object which would allow its inclusion in our statistical sample, and it is left out. All other objects reclassified by Bergeron et al. (1992) have $B_{pg} \gtrsim 14.8$ and are thus beyond the magnitude cutoff used in Paper I. With the work of Fleming et al. (1986) and Bergeron et al. (1992), it now seems likely that few, if any, additional bright hydrogen-rich subdwarfs are still lurking as DA white dwarfs in the PG catalog. Furthermore, hydrogen-rich subdwarfs masquerading as lower gravity objects or as helium-rich subdwarfs appear to be rather infrequent: no star in the Moehler et al. (1990b) spectroscopic sample turned out to be a legitimate hydrogen-rich subdwarf (sdB or sdOB in the Moehler et al. 1990b system) after having been classified as either a lower gravity HBB star or a helium-rich (*sdOB*, *sdOC*, *sdOD*, in the Green et al. terminology) subdwarf in the PG survey. Finally, at least one legitimate object has escaped photometric observation because of a misprint in the PG catalog; PG 2337+070, listed by Green et al. at $B_{pg} = 15.92$, was originally listed by Green (1980) as a much brighter object ($V = 13.47$). It was not, but clearly should have been, included in our photometric survey; the availability of Green's (1980) photometry [$(b - y) = -0.01$ and $(u - b) = +0.07$] nevertheless allows us to include it in our statistical sample.

Our final procedure is to eliminate those objects which are not part of the statistically complete sample, for the reasons discussed by Green et al. Eleven such objects were found and deleted, as were four additional objects with $b > 15.0$. We are then left with a final sample of 209 hydrogen-rich subdwarf candidates, which forms the basis of this investigation. That sample is referred to as the Palomar-Green-Strömgren (PGS) sample below. The photometric properties of the PGS sample are displayed in Figure 1, where we show the measured photographic magnitude, B_{pg}, as a function of the photoelectric Strömgren b magnitude, as well as the usual two-color diagrams $(u - b)$ versus $(b - y)$, c_1 versus $(b - y)$, and m_1 versus $(b - y)$. Figure 1*a* suggests that our statistical sample contains most of the PG subdwarfs brighter than $b \sim 14.5$, and that it should, down to that limit, be as complete as the PG survey itself. The cumulative surface density of stars within our sample is shown in Figure 2*a*, as a function of B_{pg}. We also display the surface density, based on the count slope derived by Green et al., for what they call sdB stars—a sample which includes the *sdB*, *sd*, and *sdB-O* spectral classes of the PG survey. The two sets of cumulative surface density match fairly well if we consider the following: first, we used a somewhat different, and arguably cleaner, sample of objects, initially larger since it included 47 additional *sdOA* and *sdOB* stars observed in Paper I, from which many undesirable objects were later deleted, as described in Paper I and above. Second, our surface densities are based on actual star counts for $B_{pg} \leq 14.6$, while the displayed Green et al. densities are fitted to counts in the range $14.4 \leq B_{pg} \leq 16.4$ and extrapolated (as in their Fig. 2) down to $B_{pg} = 13.0$. On that basis, we find the agreement between these cumulative surface densities entirely satisfactory.

[3] In accord with the convention introduced in Paper I, the PG classes, which are described in detail by Green et al., are italicized in the present paper to distinguish them from other classifications found in the literature. Note in particular that the recent spectral reclassification work of Moehler et al. (1990b) and Saffer et al. (1994) generally relies on data of much higher signal-to-noise ratio and spectral resolution than the classification spectra of the PG survey.

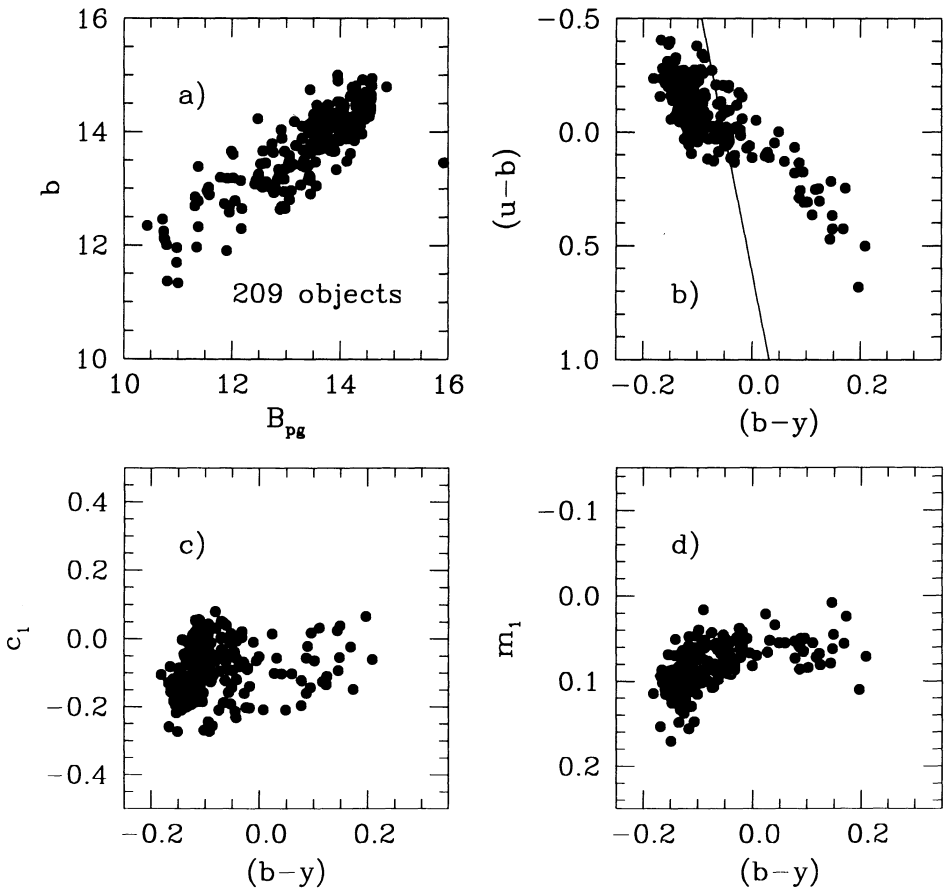

FIG. 1.—Photometric properties of our pared-down sample of 209 objects brighter than $b = 15.0$. (*a*) Strömgren b magnitude as a function of photographic B magnitude of Green et al. (1986). The cutoff near $B_{pg} \sim 14.6$ is the limiting magnitude adopted for inclusion in the photoelectric study of Paper I. Note that PG stars already in the sample of Bergeron et al. (1984) had been observed photoelectrically irrespective of their photographic magnitude. The object at $B_{pg} = 15.92$ is PG 2337+070, whose photographic B magnitude is erroneous in the PG catalog (see § 2.2). (*b*) Plot of $(u - b)$ vs. $(b - y)$. The solid line represents the arbitrary boundary to the right of which $T_{(u-b)}$ rather than $T_{Q'}$ is used to determine $T_{\rm eff}$ (see § 3.1). (*c*) Plot of c_1 vs. $(b - y)$. (*d*) Plot of m_1 vs. $(b - y)$.

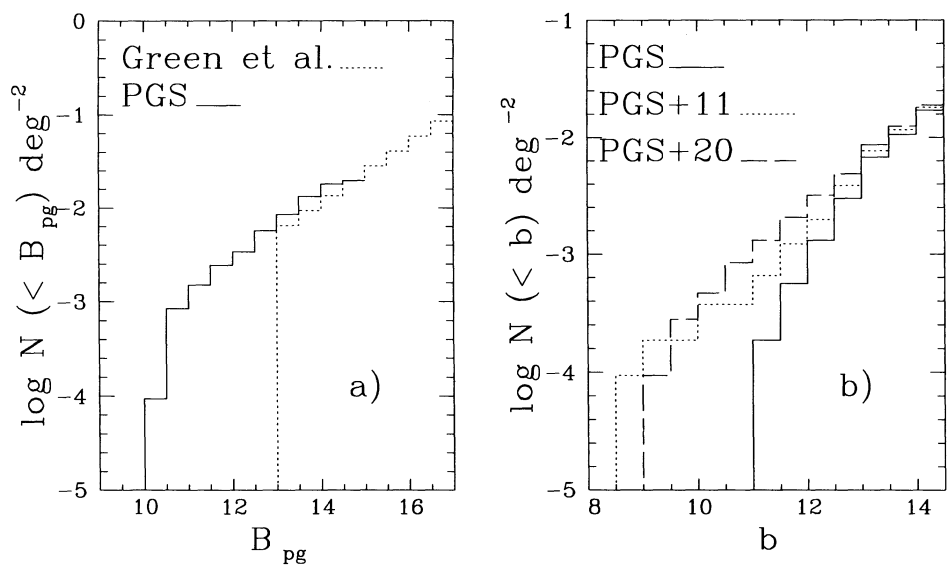

FIG. 2.—Cumulative surface density of hot, hydrogen-rich subdwarfs as a function of apparent magnitude. (*a*) As a function of B_{pg} for our sample of 209 objects (PGS) and for that of Green et al. (1986). For this figure, the erroneous B_{pg} value of PG 1033+201, given by Green et al. as $B_{pg} = -1.16$, has been replaced by its broadband value, $B = 15.45$. (*b*) As a function of photoelectric b magnitude. We show here our initial sample of 209 objects (labeled PGS), the sample augmented with the additional 11 objects found in Kilkenny et al. (1988), labeled PGS + 11, and the sample augmented with 20 objects to which were assigned average values of colors and Galactic latitude (see text), labeled PGS + 20.

With respect to completeness, Moehler et al. (1990a) have recently raised the possibility that the PG survey might not be as complete as advertised for bright magnitudes, because of plate saturation effects. Their argument is based on the absence, in the PG sample, of the rather bright sdB stars HD 4539 ($V = 10.32$) and PHL 1079 ($V = 13.38$), which figure in the catalog of spectroscopically identified hot subdwarf stars of Kilkenny, Heber, & Drilling (1988) and which lie in PG fields selected by Moehler et al. Should the PG survey be that incomplete at bright magnitudes, the number of bright subdwarfs missed in our work should be much larger, since our statistical sample covers one-quarter of the whole sky, instead of the ~ 712 deg^2 of the Moehler et al. investigation. This is an important issue, which we address in some detail below.

3. DETERMINATION OF PHYSICAL PARAMETERS

An essential ingredient in the determination of the space density of subdwarf stars is to obtain distance estimates for individual objects. This is usually accomplished by *assuming* an average M_V for all the objects, or by determining individual M_V values through model atmosphere determinations of effective temperatures and surface gravities. Because of the sheer size of the sample under investigation, accurate individual values for these parameters cannot be obtained. Rather, approximate ways have been devised to determine these parameters. Note that the largest source of uncertainty in the determination of individual distances arises from the surface gravity.

3.1. *Effective Temperature*

Even in the absence of ultraviolet spectrophotometry or optical spectra, fairly accurate values of the effective temperature can be obtained from a calibrated reddening-free color index constructed from the Strömgren colors of Paper I. We use here the index Q' defined by Bergeron et al. (1984), namely, $Q' = (u - b) - 1.56(b - y)$. It is similar to that introduced by Strömgren (1966). That index is calibrated here with unpublished model atmosphere calculations appropriate for pure hydrogen atmospheres at $\log g = 5.5$. Note further that, as emphasized recently in Paper I (see also Saffer et al. 1994), the transformation to a calibrated system of the colors which enter the calculation of Q' represents an important uncertainty in the determination of temperatures based on photoelectric photometry. We consider here the transformations of Olson (1974), based on scans of main-sequence stars, and those of Schulz (1978), based on white dwarf energy distributions. They are discussed and compared in detail in Paper I. In general, effective temperatures based on the Olson transformations are higher that those derived on the basis of the Schulz transformations, by amounts which can range from 2000 K, near 25,000 K, to 8000 K near 40,000 K (Paper I). In principle, a way to sort out these transformation problems for hot subdwarfs would be to compare the temperature estimates based on Q' only with those based on detailed model atmosphere analyses, where the effective temperature is determined from optical or ultraviolet spectrophotometry, as well as from optical photometry. However, there may well remain systematic differences between atmospheric parameters obtained in the analyses of Heber et al. (1984), Heber (1986), Moehler et al. (1990a), Theissen et al. (1993), Saffer et al. (1994), and Allard et al. (1995). Until these differences can be sorted out, there is no legitimate way to choose between the Olson or the Schulz transformations for hot subdwarfs. Both should be, and are, considered here, and the differences associated with these problems must be considered as an unavoidable uncertainty at this stage.

In addition to the problem of the calibration of the $T_{\rm eff}$ versus Q' relation, another problem appears in using a large sample of photoelectric colors. This is highlighted in Figure 1*b*, where we present the complete photometric data used here in the form of a two-color diagram. Allowing for a small amount of interstellar reddening, most of the stars observed in Paper I follow a fairly well-defined sequence in that diagram. However, several stars do show an apparent reddening in $(b - y)$ which places them to the right of the sequence. Allard et al. (1994; see also Theissen et al. 1993) demonstrated that many of these stars were likely to be reddened by a cool main-sequence companion. In particular, we find—on the basis of their analysis—that all the objects for which they secured *BVRI* photometry and which are located, in a Strömgren two-color diagram, to the right of an arbitrary boundary (shown in Fig. 1*b*) defined by $(b - y) = 0.083(u - b) - 0.051$ are most likely composites. Thus, because the $(u - b)$ color index is less affected by the possible presence of a cool companion, we used a temperature determination based only on $(u - b)$, rather than on Q', for those hot subdwarfs in our statistical sample which are located to the right of the boundary described above. All in all, this technique was used for 54 of the 209 objects which constitute our sample.[4]

To determine an effective temperature for this subsample of stars, we first calibrated the $T_{(u-b)}$ versus $T_{Q'}$ relation with 157 stars brighter than $b = 15.0$ located to the left of the boundary, where no companions are expected. These calibrations are shown in Figure 3. Because our program stars are located at high Galactic latitude and are thus only slightly reddened, we found, not surprisingly, a fairly tight relation between these two quantities, namely,

$$T_{Q'} = 1.008\,T_{(u-b)} + 558 \text{ K} \quad (1a)$$

for the Olson transformations, and

$$T_{Q'} = 0.921\,T_{(u-b)} + 525 \text{ K} \quad (1b)$$

for the Schulz transformations. Once $T_{(u-b)}$ is obtained from our sequence of model atmospheres, it is corrected, with the use of equation (1), to a standard $T_{Q'}$.

3.2. *Surface Gravity*

Individual determinations of surface gravity were, at the time this work was carried out, available only for small subsamples of PG stars. Moehler et al. (1990a) presented results of accurate $\log g$ determinations for a sample of 36 of these objects. A later companion sample, studied by Theissen et al. (1993), yielded individual values of $\log g$ for 12 additional PG stars with well-determined parameters. More recently, after this analysis was completed, Saffer et al. (1994) presented $\log g$ values for a larger sample of 68 stars, several of them in common with the work of Moehler et al. Similarly, the sample of hydrogen-rich subdwarf candidates being analyzed by

[4] Our estimates of d for these objects ignore the influence of two residual effects associated with the presence of a companion: first, that associated with the neglect of the small contamination of $(u - b)$, which affects our estimates of $T_{\rm eff}$ snd H_{5500}; and second, that associated with our use of a contaminated y magnitude to estimate f_{5500} in eq. (2). We estimate that, for typical parameters of both the subdwarf and the late-type companion, our neglect of each of these effects leads to the distance to the object being underestimated by $\sim 5\%$.

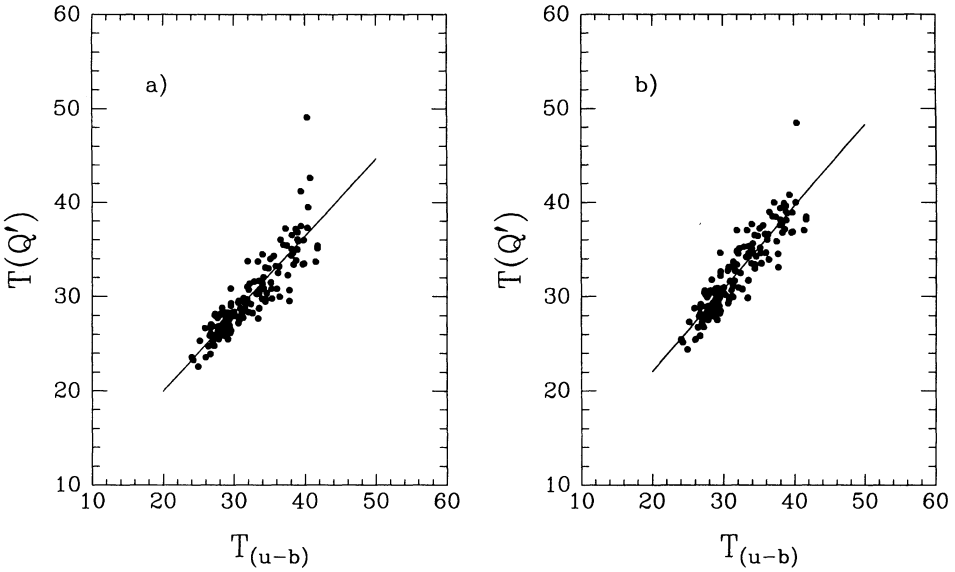

FIG. 3.—Linear regression between $T_{(u-b)}$ and $T_{Q'}$ for the 157 objects with $b \leq 15.0$ which figure to the left of the arbitrary boundary indicated in Fig. 1*b* (see text). (*a*) For the calibration of $T_{Q'}$ based on the work of Schulz (1978); (*b*) for the calibration based on the work of Olson (1974).

Allard et al. (1995; also Allard 1986) contains more than 40 PG stars, but many are also in common with the samples studied in the three investigations mentioned above. Hence, even today, it remains unrealistic to hope for *individually determined* gravities for our complete statistical sample of 209 objects. We were thus led to consider, below, several different methods to assign approximate values of log g to the stars of our sample, methods which were generally based on the *average* properties of the small samples of sdB stars for which detailed analyses were available.

A central ingredient in two of these methods is the average gravity of hot, hydrogen-rich subdwarfs. This value can be estimated on the basis of past investigations. Thus, the results of Heber et al. (1984) and Heber (1986) yield $\langle \log g \rangle = 5.50$, $\sigma = 0.29$ for a sample of 15 objects culled from various sources. In the Moehler et al. (1990a) homogeneous sample of 37 objects, the mean log g is 5.25, with a standard deviation $\sigma \sim 0.25$ dex and a typical uncertainty of 0.2 dex on individual values. The companion sample of 16 stars of Theissen et al. (1993) yields $\langle \log g \rangle = 5.32$, $\sigma = 0.27$. However, the sample of Saffer et al. (1994) yields a somewhat larger $\langle \log g \rangle = 5.76$, with a standard deviation of ~ 0.21 dex. This larger average gravity can, according to Saffer et al., be traced back to two causes: first, earlier investigations (e.g., Moehler et al. 1990a) made use of a color-effective temperature calibration which is not internally consistent with the spectroscopic calibration of Saffer et al.; second, the use of a restricted number of lower Balmer lines in the estimation of log g by Moehler et al. and their predecessors leads to a less accurate determination of the surface gravity, as compared, e.g., to the Saffer et al. investigation, which makes use of lines up to H9. Even more recently, however, a spectroscopic analysis of a sample of hydrogen-rich subdwarf candidates by Allard et al. (1995) yields $\langle \log g \rangle = 5.37$ with $\sigma = 0.51$; these values are based on an analysis relying on Hβ to Hδ only, but without any use of a color-effective temperature calibration. Thus, despite residual systematic differences between these analyses which may need to be explored further, there is a general consensus that sdB stars have $5.0 \lesssim \log g \lesssim 6.0$. Note that theoretical evolutionary tracks for extended horizontal-branch stars suggest that log g varies with $T_{\rm eff}$ (see, e.g., Caloi 1989).

On the basis of these considerations, we have used four different methods to assign surface gravities to individual objects in our sample, and complete sequences of calculations were carried out for each method. The first sequence, called the "C" sequence, consists of assigning a constant surface gravity to all program stars. We chose this value to be log $g = 5.25$, on the basis of the earlier estimates which placed the average gravity of sdB stars nearer that value. The constant-gravity sequence is probably the most unrealistic among those we consider. A second sequence, termed "GS," mimics the Greenstein & Sargent (1974) method[5] for assigning log g values (log $g\theta^4 = 2.3$). Note that this method yields average properties for a given sample which are quite reasonable: we applied it to the sample of 37 stars of Moehler et al. (1990a) and found $\langle \log g \rangle = 5.22$ with a standard deviation of $\sigma = 0.15$. Thus, the GS technique yields an average gravity similar to that determined directly by Moehler et al., but appears to underestimate the standard deviation of the sample. However, because this scheme has been used in some previous investigations of the statistical properties of sdB stars (e.g., Green & Liebert 1987), we adopt this sequence here as our reference sequence. In the last two sequences, called "R_1" and "R_2," we assigned randomly chosen individual log g values; the log g values were sampled from a Gaussian distribution centered on log $g = 5.25$, of standard deviation $\sigma = 0.25$, and extending 3 σ on each side of the maximum. R_1 and R_2 refer to two different series of random numbers.

3.3. *Distance Determination*

Individual distances, d, are obtained directly from

$$d = 3.241 \times 10^{-19} \left[\frac{4\pi G M H_{5500}}{g f_{5500}} \right]^{1/2} \text{pc} , \qquad (2)$$

[5] The soundness of the Greenstein & Sargent (1974) log $g\theta^4$ = constant relation is confirmed by the analysis of Saffer et al. (1994), who derive a slightly larger constant (2.64) on the basis of their sample of 68 hydrogen-rich subdwarfs.

TABLE 1

MEAN M_V AND STANDARD DEVIATION

Sequence (b_{lim} = 14.5)	Transformation	M_V	σ_{M_V}
C	Schulz	3.53	0.37
GS.....	Schulz	3.70	0.52
R_1	Schulz	3.48	0.73
R_2	Schulz	3.54	0.73
C	Olson	3.37	0.38
GS.....	Olson	3.93	0.51
R_1	Olson	3.32	0.74
R_2	Olson	3.38	0.73

where H_{5500} and f_{5500} are, respectively, the Eddington flux at 5500 Å computed for a given $T_{\rm eff}$ and log g from models similar to those of Wesemael et al. (1980), and the flux detected at the top of the Earth's atmosphere at the same wavelength. Other symbols have their usual meanings. The flux is obtained from the Heber et al. (1984) relation, whereby $m_y = 0.000$ corresponds to 3.60×10^{-9} ergs cm^{-2} s^{-1} Å^{-1}. The height of each star above the Galactic plane then follows from $z = d \sin b$, where b is the Galactic latitude.

A log g error of the order of the standard deviation adopted for our distribution (0.25 dex) leads to a 35% error on d. Otherwise, the most important uncertainty is that associated with the assumed stellar mass. Following Moehler et al. (1990a), we adopt a constant value of $0.5 \pm 0.1\ M_\odot$. This 20% uncertainty on the stellar mass translates into an additional 10% uncertainty on d. A 5% uncertainty must also be added to account for the $T_{\rm eff}$ uncertainty which affects H_{5500}, and for the error on the Strömgren y magnitude, which affects f_{5500}. The global effect is to produce a 50% uncertainty on d and z, an estimate comparable to that of Moehler et al.

With the distance d determined directly from $T_{\rm eff}$ and log g, the absolute magnitude M_b, used in the statistical analyses, can be computed straightforwardly from

$$M_b = m_b + 5 - 5 \log d\ , \tag{3}$$

where d is expressed in parsecs and where we have neglected interstellar extinction altogether, as seems reasonable for a sample located at high Galactic latitudes. And although M_V is not used directly in our procedure, a similar equation can be used to compute that quantity as well, in order to compare the M_V distribution for the 209 stars of our sample with those derived in previous investigations. The resulting mean value and standard deviation depend both on the adopted method for assigning log g (either the C, GS, R_1 or R_2 sequences described above), and on the particular photometric calibration used (either Schulz 1978 or Olson 1974). They are given in Table 1. Our reference sequence, the GS sequence with Schulz calibration, has a mean of $\langle M_V \rangle = 3.70$, a value which should be compared with the following mean values derived in recent analyses: the value extracted from Greenstein & Sargent (1974), $\langle M_V \rangle = 3.14$, $\sigma = 0.76$, based on the 26 sdB stars with reliable M_V values in their Table A3; $\langle M_V \rangle = 3.85$, $\sigma = 0.60$, for the eight objects of Heber et al. (1984); $\langle M_V \rangle = 4.41$, $\sigma = 0.31$, for the seven new, single objects analyzed by Heber (1986); a mean of 5.0–5.3 derived by Downes (1986); $\langle M_V \rangle = 3.53$, $\sigma = 0.52$, for the 37 objects studied by Moehler et al. (1990a); and a range of 4.3–4.5 derived by Liebert, Saffer, & Green (1994) for three B subdwarfs in the old, metal-rich Galactic cluster NGC 6791.

4. DETERMINATION OF THE SPACE DENSITY

4.1. *Some General Considerations*

The availability of a large, magnitude-limited sample gives us the opportunity to derive statistical properties of sdB stars. Quite generally, the completeness of a sample can be estimated by means of the V/V_m test, as suggested by Schmidt (1968). V represents here the volume defined by the distance to an object within the survey, while V_m is the volume defined by the maximum distance to which the same object would be detected, given the magnitude limit of the survey. If the objects are uniformly distributed, the value of $\langle V/V_m \rangle$ for the survey should be 0.5. For a nonuniform distribution, the same procedure can be applied to test for completeness, provided the respective volumes are weighted by the density distribution. As an illustration, the definitions of the volumes in the particular case of a barometric law of density characterized by a scale height z_e are

$$dV' = dV \exp(-z/z_e) \tag{4a}$$

and

$$dV'_m = dV_m \exp(-z/z_e)\ . \tag{4b}$$

Note that the V'/V'_m test can be applied with V' and V'_m *only if the parameter* z_e *is known.* Alternatively, if a given sample is known to be complete, parameter space can be searched for the value of z_e which yields a $\langle V'/V'_m \rangle$ near 0.5. We shall use this procedure here. Once z_e is determined, we can proceed with the calculation of the space density, D_0, which also depends on the assumed density distribution. Schmidt's (1975) method, which will be used here, consists of summing the $1/V'_m$ for each star of a complete sample, where V'_m is the maximum density-weighted volume accessible to each object in the survey.

Given the large number of objects in our survey, it is possible to use here as well an alternative approach to determine both scale height and space density by straightforward fits to the observed number of stars as a function of z. Values of the scale height and D_0 can be adjusted in the model stellar distribution to force it to match the observed $N(z)$ variation. This procedure permits an independent, and simultaneous, determination of the scale height and space density, which will be compared below to the values generated within the V'/V'_m test and with Schmidt's $1/V'_m$ method.

One of the main advantages of having a large sample of objects reaching down to fairly faint magnitudes is our ability to simulate smaller subsamples reaching down to various limiting magnitudes. Since we have accurate photoelectric colors at our disposal, we use the Strömgren b magnitude to define the magnitude cutoff of our various subsamples. We introduce five such subsamples, with limiting magnitudes of 13.0 (32 stars), 13.5 (72 stars), 14.0 (113 stars), 14.5 (182 stars), and finally 15.0 (the full sample of 209 stars). The first three subsamples are certainly as complete as the original survey itself, the fourth one most likely is (see § 2.2), while the last one clearly is not. The consistency between the values of the scale height and density determined for samples reaching down to different limiting magnitudes provides us with a valuable way of estimating the significance of the derived parameters.

4.2. *Model Stellar Distributions*

The radial brightness profile of the disk of a spiral galaxy follows a simple barometric law as a function of R, the distance to the Galactic center (Freeman 1970). With a constant M/L

ratio, this can be transformed into a stellar density law in the disk of the form $D(R) = D_0 \exp(-R/R_0)$. The disk scale length is estimated to be 5.5 ± 1.0 kpc (van der Kruit 1986). At the solar radius (8.5 ± 1 kpc; Binney & Tremaine 1987), the density $D(R)$ varies by less than 25% for variations in R on the scale of 1 kpc. Since the distances from the Sun, projected onto the Galactic plane, are always less than 1 kpc, even for our most remote objects, we can safely ignore the radial density gradient.

As far as the vertical distribution of stars above the plane is concerned, the situation is much less clear. It is frequently assumed that the vertical dependence of the density function can be described, in the same way as the radial dependence, by a simple barometric law as a function of z, the height above the plane (e.g., Bahcall & Soneira 1980). Thus,

$$D = D_0 \exp(-z/z_e), \quad (5)$$

where D_0 is the local space density in the disk and z_e is the exponential scale height. However, it is well known (Mihalas & Binney 1981) that this law does not fit very well the true distribution near the Galactic plane, and that a Gaussian law would be more appropriate. Following Freeman's (1978) suggestion to fit the z distribution by that of a locally isothermal sheet, van der Kruit & Searle (1981) adopt the following vertical space density function:

$$D = D_0 \operatorname{sech}^2(z/z_0), \quad (6)$$

where z_0 is the characteristic height of the distribution. This distribution has two limits of interest:

$$z/z_0 \ll 1: \quad \operatorname{sech}^2(z/z_0) \sim \exp(-z^2/z_0^2) \quad (7a)$$

and

$$z/z_0 \gg 1: \quad \operatorname{sech}^2(z/z_0) \sim \exp(-2z/z_0). \quad (7b)$$

The first limit is the Gaussian dependence mentioned earlier, while the second one corresponds to an exponential dependence with a scale height of $z_e = z_0/2$.

Van der Kruit & Searle (1981) estimate z_0 in the solar neighborhood to be $\sim$600–700 pc, a value consistent with the exponential scale height of late-type stars of 300–400 pc derived by Bahcall & Soneira (1980). They also find that values of z_0 between 600 and 900 pc describe adequately the disks of various spiral galaxies.

However, it must be stressed that van der Kruit & Searle's studies were done in the optical, and that the vertical profiles were derived and modeled away from the plane to avoid the dust lane at small z. But, as can be seen in equations (5) and (7b), both the barometric law and the sech^2 z law look similar at large z and are only different for $z \to 0$. Near the plane, the differences between the two distributions are a factor of $\sim$4 in density and $\sim$33% in stellar velocity dispersion.

Wainscoat, Freeman, & Hyland (1989) have studied, in the near-infrared, the vertical profiles of IC 2531, an edge-on galaxy similar to our own. That galaxy has also the advantage of having a low far-infrared flux so that the contamination of the old disk light by young stars is minimal. They found that the z dependence of the light in IC 2531, particularly in the redder passbands, which are less affected by absorption, has an excess at small z over the isothermal model for the old disk proposed by van der Kruit & Searle (1981), and appears to be better fitted by an exponential.

In fact, the exact dependence of the z distribution of the old disk distribution in external galaxies (and our own Galaxy) is far from being settled. In a more recent paper, van der Kruit (1988) conceded that the sech^2 law was a bad approximation of the z distribution at small z. That revision was based not only on Wainscoat's results for IC 2531 but also on studies in our own Galaxy, such as the one by Fuchs & Wielen (1987) which showed that there is a significant gradient in the mean velocity dispersion with distance from the Galactic plane, or the star count studies of Gilmore & Reid (1983) which show that the space density of the old disk population follows an exponential above 100 pc from the plane.

However, the exponential law is not free from problems, the most serious being the predicted gradient of the stellar velocity dispersion, which is much stronger than what is seen in samples of old disk stars (Bahcall 1984a, b). In the light of all those studies, van der Kruit (1988) proposed an intermediate distribution in sech z (see also Barnaby & Thronson 1992) which is a compromise between the two main contenders for the z density distribution.

5. RESULTS FOR THE PGS SAMPLE

5.1. *Test of a Uniform Distribution*

While current evidence suggests that hot subdwarf stars are not distributed uniformly in the direction perpendicular to the Galactic plane (Green et al. 1986; Green & Liebert 1987), it is instructive first to consider the simple-minded model of a uniform distribution. We have at our disposal five magnitude-limited subsamples of subdwarf stars, for which we can carry out a V/V_m test under the assumption of a uniform distribution in z. Whether a given, complete subsample shows a departure from a uniform distribution depends on the scale height of the stellar distribution. In particular, for a complete subsample characterized by the average height $\langle z \rangle$ of its members above the plane, a value of $\langle V/V_m \rangle$ less than 0.5 signals a breakdown of the assumption of a uniform distribution on the scale of $\langle z \rangle$.

Table 2 summarizes the results of these tests. Looking first at the three fainter bins, we find values of $\langle V/V_m \rangle$ becoming increasingly smaller than 0.5 as $b_{\rm lim}$ increases. As mentioned previously, this is likely to be the signature of the nonuniform vertical distribution of hot subdwarfs in the solar neighborhood on the scale of $\langle z \rangle$. From it, we deduce a mild constraint on the characteristic height of the distribution of these objects: with geometrical effects appearing unambiguously in the $b_{\rm lim} = 14.0$ bin, the characteristic height of the distribution of subdwarfs must be of the order of, or smaller than, the average $\langle z \rangle$ value for the subsample reaching that magnitude, which we calculate to be of the order of 660–780 pc. Note that the very low value of $\langle V/V_m \rangle$ for the last ($b_{\rm lim} = 15.0$) bin does reflect departures from a homogeneous distribution as well as the severe incompleteness of this deep survey.

TABLE 2

V/V_m TEST OF A UNIFORM DISTRIBUTION

$b_{\rm lim}$	$N_{\rm star}$	$\langle V/V_m \rangle$	σ[a]	$\langle z \rangle$ (pc)
13.0.....	32	0.55	0.05	480
13.5.....	72	0.53	0.03	570
14.0.....	113	0.44	0.03	655
14.5.....	182	0.42	0.02	780
15.0.....	209	0.27	0.02	830

[a] Defined as $\sigma = (12N_{\rm star})^{-1/2}$, as in Green 1980.

Proceeding now to the two brightest bins, we find that the values of $\langle V/V_m \rangle$ for those bins are consistent, within the uncertainties (evaluated as in Green 1980), with a value of 0.5. This implies one of two things: taken at face value, the consistency of the $\langle V/V_m \rangle$ value for those samples with that of a homogeneous distribution suggests that the scale height of the distribution must be *considerably larger* ($\gtrsim 1$ kpc) than the average value of z stars in the samples, namely, 480–570 pc (see Table 2). On the other hand, if one favors a smaller scale height (as do most studies today) for the stellar distribution, the only way to obtain $\langle V/V_m \rangle = 0.5$ is to assume that the $\langle V/V_m \rangle$ values are skewed *by a deficiency of bright objects in the PG survey*. Either way, then, there is a problem.

5.2. *A First Look at the Incompleteness at Bright Magnitudes of the PG Survey*

As mentioned previously, Moehler et al. (1990a) have argued that the completeness of the PG survey is smaller than advertised at bright magnitudes. The results of our V/V_m tests for the two brightest subsamples certainly seem to corroborate that result (although an exponential scale height $\gtrsim 1$ kpc could also account for the results found). Clearly, the interpretation of the results of the V/V_m test for the brightest subsamples depends critically on their completeness.

How many bright objects could have been missed in the PG sample? A crude estimate of that number can be obtained by extending the results of Moehler et al. (1990a) to a larger region of the sky. Accordingly, we have searched the catalog of spectroscopically identified hot subdwarfs of Kilkenny et al. (1988) for bright hydrogen-rich hot subdwarfs *not recovered in the PG catalog*, but nevertheless located in fields which are part of our complete sample. While this procedure carries some uncertainties, we believe we have identified 11 such objects, which were missed by the PG survey.[6] Of course, there is no reason to believe either that the Kilkenny et al. (1988) catalog is complete with respect to bright, hydrogen-rich subdwarfs over the more than 10,000 deg^2 of the PG survey. But, clearly, our rudimentary search suggests that there might indeed be a fair number of hydrogen-rich subdwarfs missing at bright magnitudes in the PG catalog: our estimates for the number of missing objects range from 30, based on a scaling of the two stars reported by Moehler et al. (1990a) in their search of 712 deg^2 (15 if we exclude PHL 1079, as suggested here), to 11, on the basis of our own accounting in the Kilkenny et al. (1988) catalog.

Given this uncertainty, it became of interest to explore (see § 6.1) the effects brought about by the inclusion of additional bright objects to our original sample. We shall consider two cases: first, the inclusion of the 11 objects identified above; and, second, the addition of a total of $\sim$20 bright objects below $b = 12.5$ to our PGS sample of 209 stars. In the former case, the actual Galactic latitudes and colors, when available, of the 11 objects were used to include them in the augmented sample. In the latter case, the 20 objects were all assigned the same colors [$(u - b) = -0.073$; $(b - y) = -0.076$, the average colors in our sample of 209 objects], and the same Galactic latitude ($\sin b = 0.75$, again the average value for the sample). The assignment of b magnitudes to individual objects was then made on the basis of our cumulative surface density of hydrogen-rich subdwarfs for the sample of 209 objects, which is shown in Figure 2*b* (labeled PGS). The logarithmic count slope between the $b = 14.0$ and $b = 14.5$ bins was simply extrapolated linearly at brighter magnitudes. Figure 2*b* shows the result of this procedure: the cumulative surface density obtained by including the 11 additional stars found in the Kilkenny et al. catalog is labeled PGS + 11, while that obtained by adding instead 20 supplementary objects is labeled PGS + 20.

5.3. *Results within the Exponential Model*

We consider here an exponential stellar distribution perpendicular to the plane. As a first step, we need to evaluate z_e, and this is accomplished by carrying out the V'/V'_m test for different values of z_e on each subsample expected to be complete. The value of z_e which gives, within the uncertainties, a $\langle V'/V'_m \rangle$ value near 0.5 for a given subsample is defined as the optimal exponential scale height for this sample.

Table 3 shows the results obtained for the GS sequence, with effective temperatures based on the Schulz (1978) calibration. For each survey down to a given limiting brightness, we give the z_e value required to satisfy $\langle V'/V'_m \rangle = 0.5$ for that survey, as well as the associated space density. For the two brightest subsamples, the $\langle V'/V'_m \rangle = 0.5$ requirement cannot be met, as even an exponential distribution with an infinite scale height, i.e., a uniform distribution, does not provide a $\langle V'/V'_m \rangle$ value of 0.5 (see Table 2). The value of z_e listed in the first two lines of Table 3 are thus lower limits obtained by requiring that the $\langle V'/V'_m \rangle$ value be within 1 σ of 0.5 (see Table 2). Values of z_e obtained from the next two brightness bins, which are still affected by the incompleteness at bright magnitudes, are in the range 800–900 pc. On the basis of these two bins, $\langle D_0 \rangle = 1.5 \times 10^{-7}$ pc^{-3}. The last bin displays an artifically smaller value of z_e, an expected result, since this sample is far from statistical completeness: to model it with an exponential distribution requires a steeply decreasing distribution or, equivalently, a small exponential scale height.

For the two subsamples down to $b_{\rm lim} = 14.0$ and 14.5, we also list the value of $\langle V'/V'_m \rangle$ which would be obtained if a value of $z_e = 250$ pc had been selected at the outset. This is a value typical of the exponential scale heights derived for these objects on the basis of restricted samples of PG stars (Moehler

TABLE 3

V'/V'_m TEST WITHIN EXPONENTIAL MODEL: GS SEQUENCE, SCHULZ TRANSFORMATION, PGS SAMPLE

$b_{\rm lim}$	z_e (pc)	$\langle V'/V'_m \rangle$	D_0 (pc^{-3})
13.0.....	$\geq$3000	0.56	0.9×10^{-7}
13.5.....	$\geq$3000	0.53	1.1×10^{-7}
14.0.....	900	0.50	1.4×10^{-7}
14.5.....	800	0.50	1.6×10^{-7}
15.0.....	400	0.50	3.1×10^{-7}
14.0.....	250	0.67	6.6×10^{-7}
14.5.....	250	0.68	8.7×10^{-7}

[6] The objects are HD 4539 ($V = 10.32$), in the PG field 172; BD +25°2534 ($V = 10.55$), in field 116; F91 ($V = 13.5$), in field 279; F108 ($V = 12.98$), in field 169; PB 5450 ($V = 13.06$), in field 169; UV 1419−09 ($V = 12.09$), in field 243; HD 149382 ($V = 8.95$), in field 266; BD +29°3070 ($V \leq 11.6$), in field 109; BD −3°5357 ($V = 9.34$), in field 162; UV 1735+22 ($V \leq 11.7$), in field 109; SA 58-327 ($B = 13$), in field 135. All these objects are located within a radius of 4°.35 of the center of the given field. Note that we recover here HD 4539, whose absence in the PG survey had already been noted by Moehler et al. (1990a), but not PHL 1079, which we find to be slightly outside field 177. The photometry listed here, and the coordinates used, are from Kilkenny et al. (1988).

et al. 1990a; Theissen et al. 1993). Our calculations show that *this value of z_e does not satisfy the V'/V'_m test for either of our two larger complete subsamples.*

To further explore to what extent an exponential distribution can reproduce the detailed $N(z)$ distribution of stars within our subsamples, we have attempted to fit, with a χ^2 technique, the observed $N(z)$ distributions to those predicted within the exponential model, treating the density D_0 and the scale height z_e as adjustable parameters. In this procedure, the number of stars at bin z_i located between z_{i-1} and z_{i+1} in a survey of n fields, each characterized by a solid angle ω_j and a central Galactic latitude b_j, is, for a given choice of D_0 and z_e,

$$N(z_i) = \sum_{j=1}^{n} \frac{D_0\,\omega_j}{\sin^3 b_j} \int_{z_{i-1}}^{\min[z_{i+1}, z_{\max}(j)]} z^2 \exp\left(-\frac{z}{z_e}\right) dz \,. \quad (8)$$

The maximum z at which field j contributes, $z_{\max}(j)$, is determined by the limiting magnitude of the survey, the Galactic latitude of the field, and the absolute magnitude of stars within it. For the specific purpose of this calculation, we assume $M_b = 3.5$ for all stars within a field, a value based on the mean value $\langle M_V \rangle = 3.56$ for all the Schulz sequences of Table 3, and on the mean color of stars in our sample, $\langle (b-y) \rangle = -0.076$.

The general χ^2 for our problem is

$$\chi^2 = \sum_{i=1}^{\mathcal{N}} \left[\frac{N(z_i) - N(z_i, D_0, z_e)}{\sigma_i} \right]^2 , \quad (9)$$

where $\mathcal{N}$ represents the number of bins, $N(z_i)$ the observed number of stars in bin z_i and $N(z_i, D_0, z_e)$ the number of stars predicted for a given D_0 and z_e, and σ_i the error on $N(z_i)$. The latter are estimated under the assumption that the observed $N(z_i)$ can be described by a Poisson distribution; thus $\sigma_i = [N(z_i)]^{1/2}$.

Sample results of these calculations are displayed in Figures 4–8 and in Table 4. We have isolated in these figures the uncertainties associated with (1) the method adopted in assigning surface gravities, (2) the color transformation used for the assignment of $T_{\rm eff}$, and (3) the depth of the subsample under consideration. In Figure 4 we display fits to the $N(z)$ distribution for the $b_{\rm lim} = 14.5$ subsample. Temperatures here are derived with the Schulz (1978) photometric transformation. The four panels show the various sequences of log g determination, namely, C, GS, R_1, and R_2, while Figure 5 displays, in the form of contour plots the confidence level associated with these fits to the $N(z)$ distribution. Figure 6 displays the differences associated with a change from the Schulz (1978) to the Olson (1974) color transformation for the $b_{\rm lim} = 14.5$ subsample and the GS and R_2 sequences. Figure 7 displays the results obtained for the GS sequence for the complete set of four magnitude subsamples, while Figure 8 displays, once again, the confidence levels associated with these fits in the (D_0, z_e)-plane. The derived values of z_e, the optimal value of the exponential scale height, and of D_0, the associated value of the space density, for all these sequences are given in Table 4.

TABLE 4

RESULTS OF TWO-DIMENSIONAL FITS WITHIN EXPONENTIAL MODEL: PGS SAMPLE

$b_{\rm lim}$	Sequence	Transformation	z_e (pc)	D_0 (pc^{-3})
14.5.....	C	Schulz	>750[a]	0.8×10^{-7}
	GS	Schulz	700	1.5×10^{-7}
	R_1	Schulz	600	1.5×10^{-7}
	R_2	Schulz	700	1.3×10^{-7}
	GS	Olson	400	3.3×10^{-7}
	R_2	Olson	1000	0.9×10^{-7}
13.0.....	GS	Schulz	>300[a]	0.9×10^{-7}
13.5.....	GS	Schulz	>800[a]	0.9×10^{-7}
14.0.....	GS	Schulz	>550[a]	1.1×10^{-7}

[a] At the 90% confidence level.

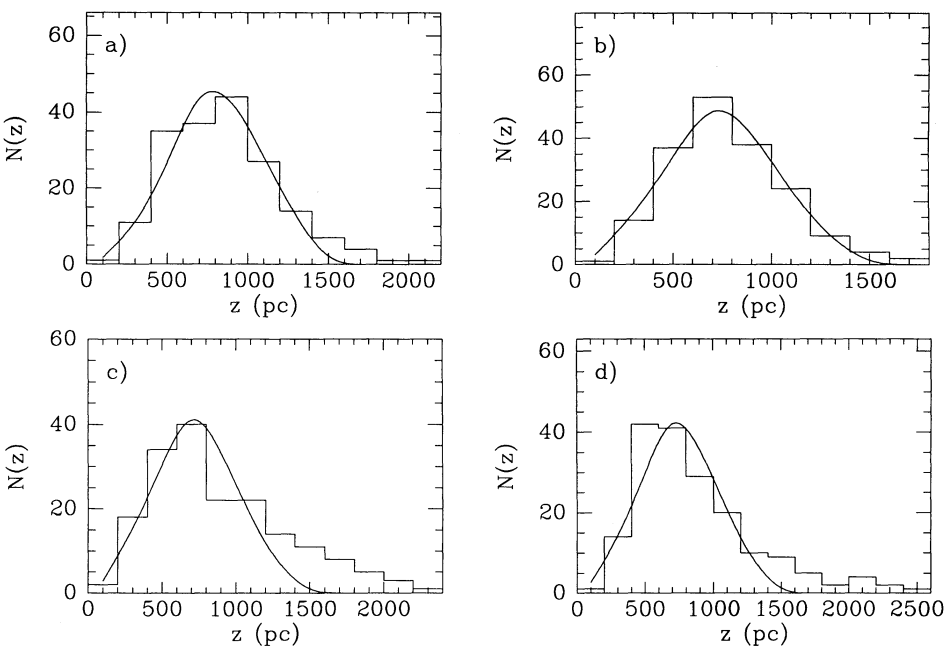

FIG. 4.—Observed (*histogram*) and best-fit (*solid line*) $N(z)$ distributions in the exponential model for the $b_{\rm lim} = 14.5$ PGS subsample. Temperatures are obtained from Q' or $(u-b)$ (see text), on the basis of the Schulz calibration. (*a*) The so-called C sequence, where surface gravities are taken to be a constant, log $g = 5.25$. (*b*) The GS sequence, where surface gravities are assigned on the basis of log $g\theta^4 = 2.3$. This is our reference sequence. (*c*) The R_1 sequence, where surface gravities are assigned randomly (see text). (*d*) The R_2 sequence, where surface gravities are assigned randomly (see text).

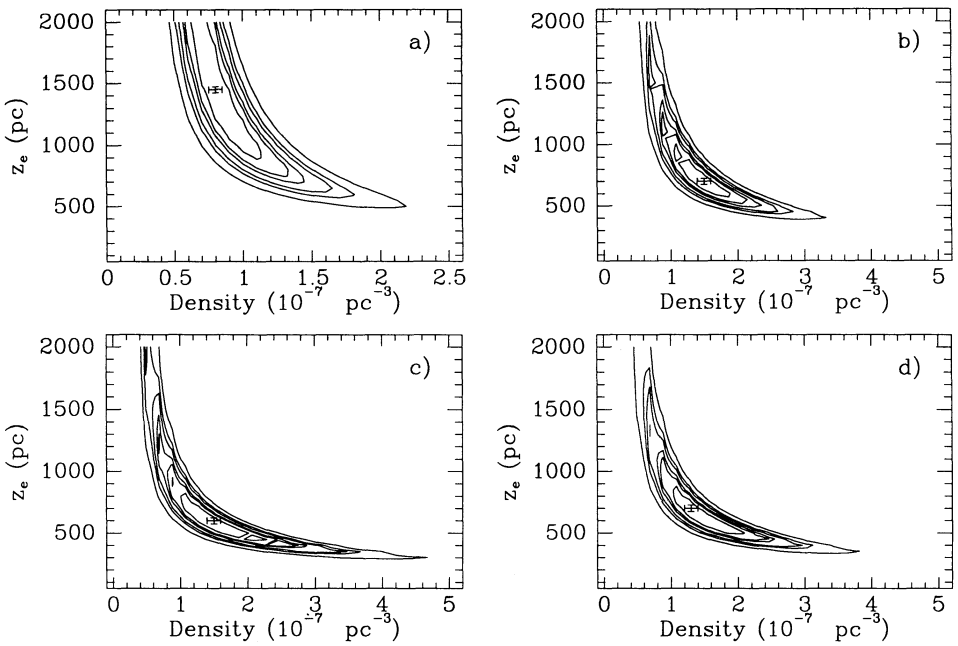

FIG. 5.—Contours of equal confidence level associated with the fit to the $N(z)$ distribution of the $b_{lim} = 14.5$ PGS subsample with an exponential distribution (Fig. 4). The contours shown are for 68.3%, 90%, 95.4%, 99%, 99.73%, and 99.99% confidence levels. The cross indicates the set of D_0 and z_e associated with the minimal deviation. These values are given in Table 3. When the 90% confidence contour remains open, only a lower limit based upon that contour is given there. Temperatures are obtained from Q' or $(u - b)$ (see text), on the basis of the Schulz calibration. (*a*) The so-called C sequence, where surface gravities are taken to be a constant, $\log g = 5.25$. (*b*) The GS sequence, where surface gravities are assigned on the basis of $\log g\theta^4 = 2.3$. This is our reference sequence. (*c*) The R_1 sequence, where surface gravities are assigned randomly (see text). (*d*) The R_2 sequence, where surface gravities are assigned randomly (see text).

Some interesting results can be extracted from an examination of Table 4. First of all, the use of different techniques to assign individual $\log g$, and thus M_V, values lead to uncertainties, within the exponential model, of a factor ~ 2 in D_0. The change in z_e is more difficult to evaluate, since the value of z_e for the $b_{lim} = 14.5$ C sequence is a lower limit only and is essentially unconstrained (a discussion of this point appears below); on the basis of the other three sequences, the uncertainty in z_e appears to be $\sim 15\%$, but the true uncertainty is likely to be much larger, perhaps as much as 50%. Furthermore, the changes brought about by different color transformations are a factor of $\lesssim 2$ both in D_0 and in z_e. Changes in the color transformation impact differently on different methods of assigning M_V. For example, in the R_2 sequence, the higher temperatures assigned with the Olson calibration simply lead to larger luminosities, larger individual distances, and thus

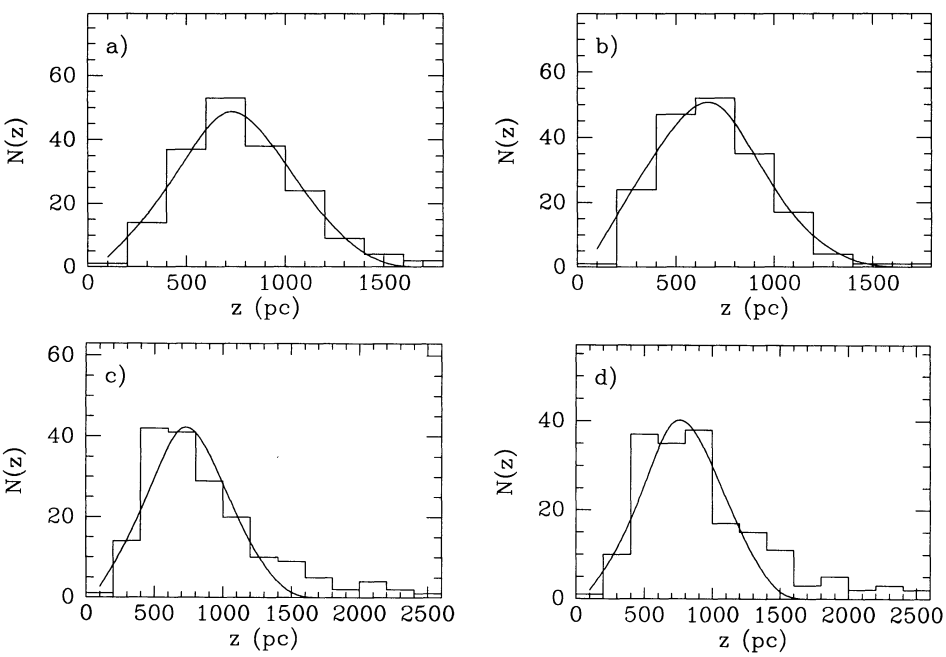

FIG. 6.—Observed (*histogram*) and best-fit (*solid line*) $N(z)$ distributions in the exponential model for the $b_{lim} = 14.5$ PGS subsample. (*a*) The GS sequence, with the Schulz calibration; this panel is identical to Fig. 4*b*. (*b*) The GS sequence, with the Olson calibration. (*c*) The R_2 sequence, with the Schulz calibration; this panel is identical to Fig. 4*d*. (*d*) The R_2 sequence, with the Olson calibration.

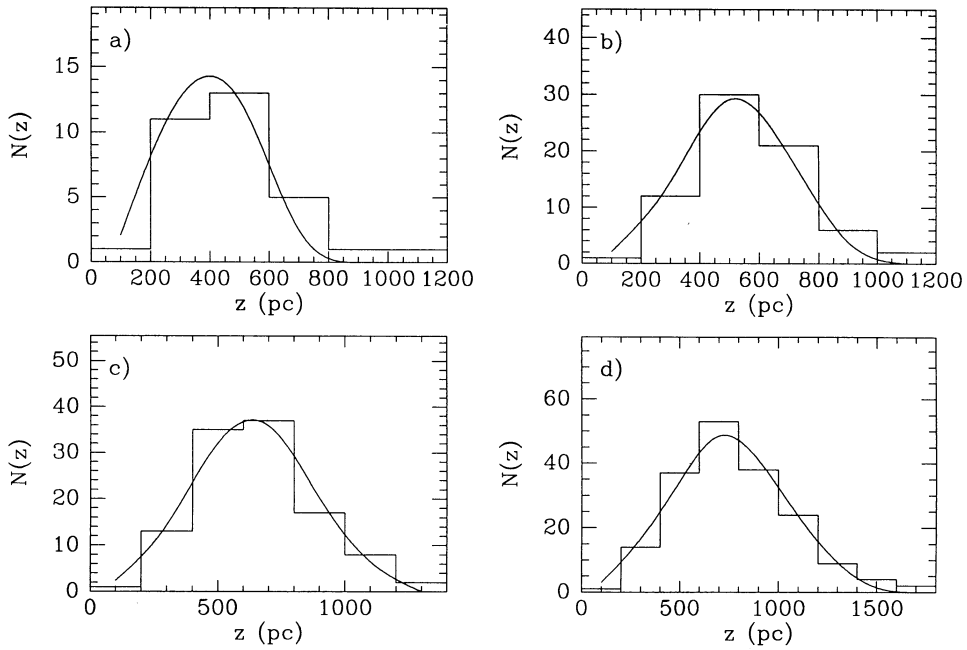

FIG. 7.—Observed (*histogram*) and best-fit (*solid line*) $N(z)$ distributions in the exponential model. Temperatures are obtained from Q' or $(u - b)$ (see text), on the basis of the Schulz calibration. This is the so-called GS sequence (see text). (*a*) The $b_{lim} = 13.0$ PGS subsample. (*b*) The $b_{lim} = 13.5$ PGS subsample. (*c*) The $b_{lim} = 14.0$ PGS subsample. (*d*) The $b_{lim} = 14.5$ PGS subsample; this panel is identical to Fig. 4*b*.

larger values of z_e and lower values of D_0. In the GS sequence, the effects are more complex, since the Olson calibration leads not only to hotter temperatures but also to larger surface gravities through the log $g\theta^4 = 2.3$ relationship. These temperature and gravity changes affect the luminosity in opposite directions, but our calculations show that the surface gravity variations dominate the luminosity changes. Hence, in the GS sequence, the luminosities are ultimately *decreased* when the Olson calibration is used; the exponential scale height z_e thus decreases, and the space density D_0 increases compared to the values determined with the Schulz calibration.

We now proceed to an examination of the sensitivity of the drived z_e and D_0 values to the limiting brightness of the sample: in this respect, our results are far from satisfactory, in the sense that—as illustrated in Figures 8*a*–8*c*—the exponential scale height is essentially unconstrained in our two-

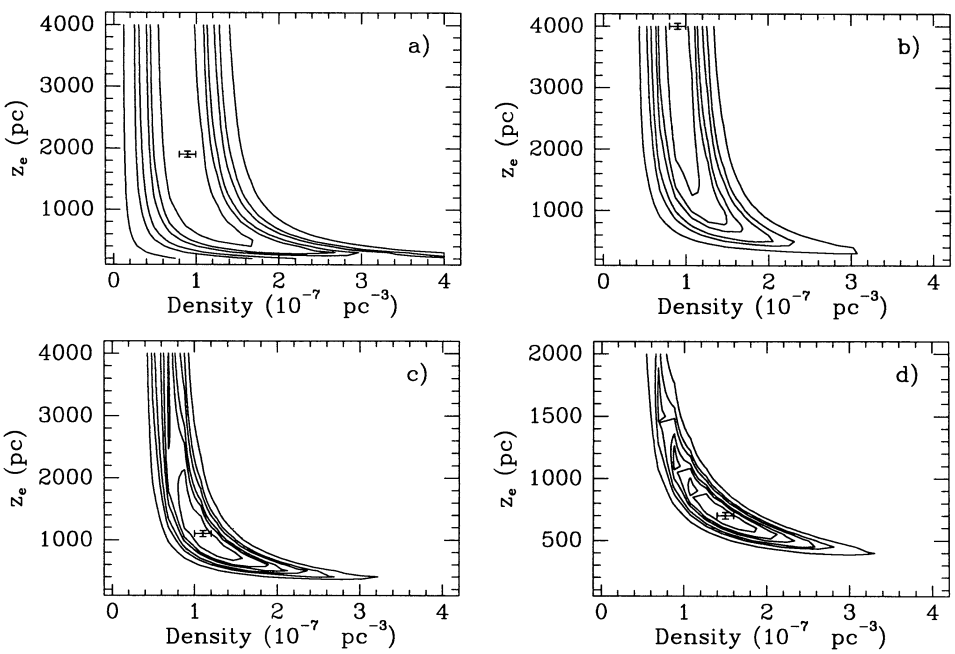

FIG. 8.—Contours of equal probability associated with the fit to the $N(z)$ distribution with an exponential model (Fig. 7). The contours shown are for 68.3%, 90%, 95.4%, 99%, 99.73%, and 99.99% confidence levels. The cross indicates the set of D_0 and z_e associated with the minimal deviation. These values are given in Table 3. When the 90% confidence contour remains open, only a lower limit based upon that contour is given there. Temperatures are obtained from Q' or $(u - b)$ (see text), on the basis of the Schulz calibration. This is the GS sequence, where surface gravities are assigned on the basis of log $g\theta^4 = 2.3$. (*a*) The $b_{lim} = 13.0$ PGS subsample. (*b*) The $b_{lim} = 13.5$ PGS sample. (*c*) The $b_{lim} = 14.0$ PGS sample. (*d*) The $b_{lim} = 14.5$ PGS sample; this panel is identical to Fig. 5*b*.

dimensional fits to the $N(z)$ distributions of the brightest bins. This is also the case (see Fig. 5*a*) with the $b_{\rm lim} = 14.5$ C sequence, where the surface gravity of all stars in the sample is assumed to be a constant. In all these cases, the contours of equal confidence level are unbounded at large values of z_e. The values given in Table 4 are lower limits on z_e based on the 90% confidence level. Note, however, that the corresponding values of D_0 remain nevertheless fairly well constrained, irrespective of the value of z_e. On the basis of our GS sequence, $\langle D_0 \rangle = 1.1 \times 10^{-7}$ pc^{-3}, with a standard deviation of 0.3×10^{-7} pc^{-3}. One way to understand this lack of sensitivity is to realize that the space density summing of the individual $1/V'_m$ contribution of each star (see eq. [4b]) becomes independent of z_e once z_e is large enough, $z_e \gtrsim \langle z \rangle$. Put differently, the boundaries of the contours are vertical lines in the (z_e, D_0) plane. Furthermore, the values of D_0 derived here are entirely consistent with the space densities derived with the V'/V'_m test in Table 3.

In many ways, our inability to constrain z_e properly on the basis of our fits to the $N(z)$ distribution is reminiscent of problems encountered earlier within the V'/V'_m formalism (Table 3), where no value of z_e, however large, could satisfy the V'/V'_m test for the brightest bins. In order to try to account for these difficulties, we explore first the possibility that the exponential distribution might not be a good representation of the vertical distribution of hydrogen-rich subdwarfs, and consider the isothermal sheet distribution introduced in § 4.2.

5.4. *The Isothermal Sheet Distribution to the Rescue?*

We next investigate the adequacy of the isothermal sheet model, given by equation (6), in satisfying the V'/V'_m test as well as to describe the observed $N(z)$ variations for our various brightness subsamples. The results of this analysis are provided in Tables 5 and 6. In Table 5 we have repeated our V'/V'_m tests with the five original brightness subsamples. The new results are clearly consistent with those of Table 3: the test cannot be satisfied for the two brightest magnitude bins, where the $\langle V'/V'_m \rangle$ value remains significantly above 0.5. For the next two bins, a value of $z_0 = 1000$ pc satisfies the test, with an associated value of the density of $\langle D_0 \rangle = 1.1 \times 10^{-7}$ pc^{-3}. The last bin, associated with the statistically incomplete survey down to $b_{\rm lim} = 15.0$, once again requires a small scale height, 650 pc, to compensate for that incompleteness.

We next consider fits to the observed $N(z)$ distribution, and again write that the number of stars at bin z_i, located between z_{i-1} and z_{i+1}, in a survey of n fields, each characterized by a solid angle ω_j and a central Galactic latitude b_j, is, for a given value of D_0 and z_0,

$$N(z_i) = \sum_{j=1}^{n} \frac{D_0\,\omega_j}{\sin^3 b_j} \int_{z_{i-1}}^{\min[z_{i+1}, z_{\max}(j)]} z^2 \,\mathrm{sech}^2\left(-\frac{z}{z_0}\right) dz \,. \quad (10)$$

TABLE 5

V'/V'_m TEST WITHIN ISOTHERMAL MODEL: GS SEQUENCE, SCHULZ TRANSFORMATION, PGS SAMPLE

$b_{\rm lim}$	z_0 (pc)	$\langle V'/V'_m \rangle$	D_0 (pc^{-3})
13.0.....	≥2500	0.56	0.8×10^{-7}
13.5.....	≥2500	0.53	0.9×10^{-7}
14.0.....	1000	0.50	1.1×10^{-7}
14.5.....	1000	0.50	1.1×10^{-7}
15.0.....	650	0.50	1.6×10^{-7}

TABLE 6

RESULTS OF TWO-DIMENSIONAL FITS WITHIN ISOTHERMAL SHEET MODEL: PGS SAMPLE

$b_{\rm lim}$	Sequence	Transformation	z_0 (pc)	D_0 (pc^{-3})
14.5.....	C	Schulz	>1000[a]	0.6×10^{-7}
	GS	Schulz	900	1.0×10^{-7}
	R_1	Schulz	750	1.0×10^{-7}
	R_2	Schulz	800	1.0×10^{-7}
	GS	Olson	650	1.6×10^{-7}
	R_2	Olson	1250	0.6×10^{-7}
13.0.....	GS	Schulz	>400[a]	0.7×10^{-7}
13.5.....	GS	Schulz	>800[a]	0.9×10^{-7}
14.0.....	GS	Schulz	>700[a]	0.9×10^{-7}

[a] At the 90% confidence level.

Sample results from these fits are shown in Figure 9, and the derived parameters are summarized in Table 6. Clearly, the use of a different model for the spatial distribution of hydrogen-rich subdwarfs has not altered the basic conclusions already reached in § 5.3: the distribution scale heights remain relatively unconstrained in studies of the first three brightness subsamples, down to $b_{\rm lim} = 14.0$, while the space density determination remains relatively insensitive to the exact value of z_0; we find, within the isothermal distribution and for the GS sequence, $\langle D_0 \rangle = 0.9 \times 10^{-7}$ pc^{-3}, with a standard deviation of 0.1×10^{-7} pc^{-3}.

6. THE CONFIRMED DEARTH OF BRIGHT OBJECTS IN THE PG SURVEY

Given (1) the results of our study of a uniform distribution in § 5.1, which argued for a likely dearth of bright objects in our statistical sample, (2) the observational evidence, presented in § 5.2, of such a paucity, and (3) the problems encountered in §§ 5.3 and 5.4 in deriving homogeneous and self-consistent values of the scale height of the distribution of hydrogen-rich subdwarfs within two distinct geometrical models, we have considered further the influence of this incompleteness at bright magnitudes on the results of our determinations of either z_e or z_0 and D_0. This has been done along the following two distinct lines: first of all, we have repeated all of our calculations with two augmented data sets, termed earlier PGS + 11 and PGS + 20, which attempt to redress the paucity of bright objects in our inital sample (termed PGS in Fig. 2*b*). As a second, alternative procedure, we have elected to impose a *bright limit* to all our statistical samples.

6.1. *The PGS + 11 and PGS + 20 Samples*

Sample results based on our use of the PGS + 11 and PGS + 20 samples are given in Tables 7–9. Table 7 shows that the improvements brought about by the inclusion of additional bright objects in our exponential description are obvious and dramatic: the requirement that $\langle V'/V'_m \rangle = 0.5$ can now be satisfied for all magnitude bins with the PGS + 11 sample, although the exponential scale heights remain poorly constrained. Only with the inclusion of 20 additional bright objects does it become possible to satisfy fairly consistently the V'/V'_m criterion, and this with exponential scale heights in the 400–500 pc range. The first bin, with $b_{\rm lim} = 13$, requires a smaller scale height, $z_e = 275$ pc. The average height $\langle z \rangle$ above the Galactic plane of stars within that bin in the PGS + 20 sample is 380 pc; in general, we found it difficult to constrain

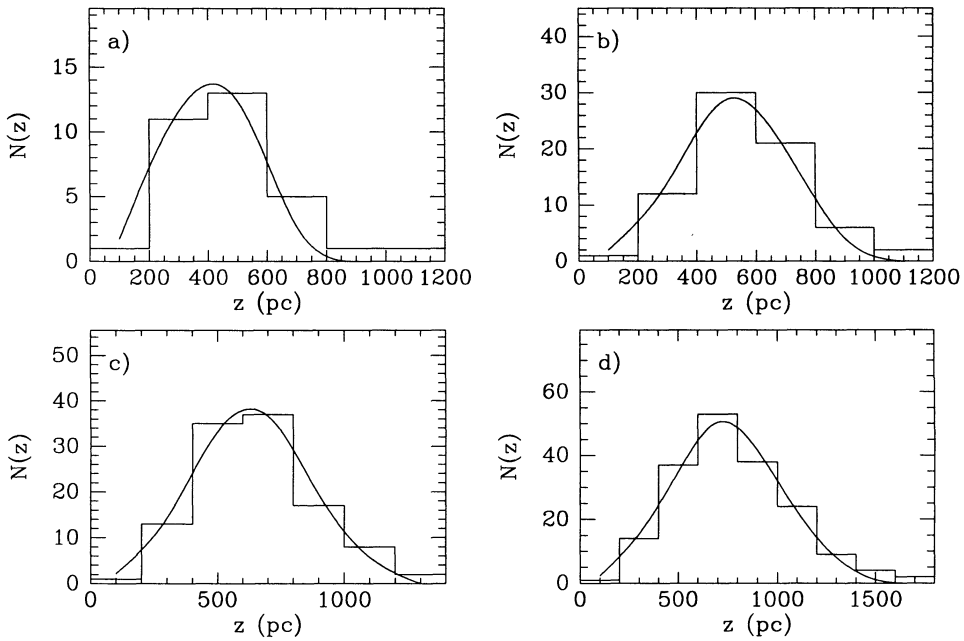

FIG. 9.—Observed (*histogram*) and best-fit (*solid line*) $N(z)$ distributions in the isothermal model for the $b_{lim} = 13.0$ PGS subsample. Temperatures are obtained from Q' or $(u - b)$ (see text), on the basis of the Schulz calibration. This is the so-called GS sequence (see text). (*a*) The $b_{lim} = 13.0$ PGS subsample. (*b*) The $b_{lim} = 13.5$ PGS subsample: (*c*) The $b_{lim} = 14.0$ PGS subsample. (*d*) The $b_{lim} = 14.5$ PGS subsample.

effectively, with stars in that bin, the exponential scale height of the distribution, since this bin barely probes into the Galaxy. Note furthermore that, for both augmented samples at $b_{lim} = 14.0$ and 14.5, the canonical value of $z_e = 250$ pc again fails to yield a value of $\langle V'/V'_m \rangle$ near 0.50. While all results in Table 7 were obtained within the exponential model, similar improvements were seen in the consistency of the results of the V'/V'_m test with those of the isothermal sheet model.

Prompted by these improvements, we have also repeated all our fits to the $N(z)$ distributions with both samples and within both exponential and isothermal geometries. Sample results are given in Tables 8 and 9 for the sample PGS + 20 only. In general, these results are more satisfactory in the sense that (1) the contours of equal confidence level now all tend to be closed, except for the $b_{lim} = 13.5$ GS sequence within both geometrical models, and (2) we now find a much improved consistency between the values of the characteristic scale height determined from the various brightness bins: including the brightest bin ($b_{lim} = 13.0$), which consistently yields a smaller scale height, and using the 90% confidence value for the $b_{lim} = 13.5$ GS sequence yields $\langle z_e \rangle = 390$ pc, with a standard deviation $\sigma = 130$ pc for the GS sequence within the exponential model. Leaving the 13.0 and 13.5 bins out, $\langle z_e \rangle = 500$ pc. For the same sequence within the isothermal sheet model, $\langle z_0 \rangle = 550$ pc, with a standard deviation $\sigma = 205$ pc with the $b_{lim} = 13.0$ and 13.5 bins, or $\langle z_0 \rangle = 725$ pc without them. The corresponding space densities, using all four bins, are $\langle D_0 \rangle = 3.1 \times 10^{-7}$ pc^{-3}, with a standard deviation of 1.4×10^{-7} pc^{-3} for the exponential distribution, and $\langle D_0 \rangle = 1.9 \times 10^{-7}$ pc^{-3}, with $\sigma = 0.9 \times 10^{-7}$ pc^{-3} for the isothermal one.

TABLE 7

V'/V'_m TEST WITHIN EXPONENTIAL MODEL: GS SEQUENCE, SCHULZ TRANSFORMATION, AUGMENTED SAMPLES

b_{lim}	z_e (pc)	$\langle V'/V'_m \rangle$	D_0 (pc^{-3})
PGS + 11 Sample			
13.0.....	≥2500	0.51	1.3×10^{-7}
13.5.....	≥2000	0.51	1.4×10^{-7}
14.0.....	600	0.50	2.2×10^{-7}
14.5.....	600	0.51	2.2×10^{-7}
14.0.....	250	0.63	7.3×10^{-7}
14.5.....	250	0.66	9.3×10^{-7}
PGS + 20 Sample			
13.0.....	275	0.50	4.9×10^{-7}
13.5.....	500	0.50	3.0×10^{-7}
14.0.....	425	0.50	3.3×10^{-7}
14.5.....	500	0.50	2.9×10^{-7}
14.0.....	250	0.58	7.8×10^{-7}
14.5.....	250	0.63	9.7×10^{-7}

6.2. *A Bright Magnitude Cutoff*

In this alternative approach, we impose a bright cutoff to all our statistical subsamples. This method, while reducing the

TABLE 8

RESULTS OF TWO-DIMENSIONAL FITS WITHIN EXPONENTIAL MODEL: PGS + 20 SAMPLE

b_{lim}	Sequence	Transformation	z_e (pc)	D_0 (pc^{-3})
14.5.....	C	Schulz	850	1.3×10^{-7}
	GS	Schulz	500	2.5×10^{-7}
	R_1	Schulz	400	2.9×10^{-7}
	R_2	Schulz	400	3.1×10^{-7}
	GS	Olson	350	4.5×10^{-7}
	R_2	Olson	550	1.9×10^{-7}
13.0.....	GS	Schulz	250	5.1×10^{-7}
13.5.....	GS	Schulz	>300[a]	2.1×10^{-7}
14.0.....	GS	Schulz	500	2.5×10^{-7}

[a] At the 90% confidence level.

TABLE 9

RESULTS OF TWO-DIMENSIONAL FITS WITHIN ISOTHERMAL SHEET MODEL: PGS + 20 SAMPLE

b_{lim}	Sequence	Transformation	z_0 (pc)	D_0 (pc^{-3})
14.5.....	C	Schulz	1150	0.8×10^{-7}
	GS	Schulz	750	1.4×10^{-7}
	R_1	Schulz	600	1.6×10^{-7}
	R_2	Schulz	600	1.8×10^{-7}
	GS	Olson	550	2.4×10^{-7}
	R_2	Olson	850	1.0×10^{-7}
13.0.....	GS	Schulz	350	3.2×10^{-7}
13.5.....	GS	Schulz	>400[a]	1.4×10^{-7}
14.0.....	GS	Schulz	700	1.4×10^{-7}

[a] At the 90% confidence level.

number of objects within each sample, avoids some of the arbitrariness associated with the addition of "missed objects" to the statistical sample. The V'/V'_m test, as well as the determination of space densities based on the summing of the $1/V'_m$ contributions, can be used here as well, provided that the volumes used are those of truncated cones.

We have chosen for this procedure a bright cutoff of $b = 12.5$, a value consistent with the 4 mag dynamic range of the IIa-O film used in the photographic survey. Note that, even at that relatively faint value, there is evidence that some stars fainter than this cutoff have been missed in the PG survey (i.e., F108, F91, PB 5450, and SA 58-327; see footnote 5). With this cutoff the $b_{lim} = 14.5$ sample, which contained 182 stars, is now reduced to 168 objects. For a typical subdwarf at $M_V = 3.5$ and at a Galactic latitude of 60°, the range of heights above the plane sampled by the range $12.5 \leq b \leq 14.5$ would be 550 pc $\leq z \leq$ 1400 pc. For our reference GS sequence based on the Schulz calibration and the $b_{lim} = 14.5$ sample, we satisfy the V'/V'_m test with an exponential scale height of $z_e = 500$ pc; the associated space density is $D_0 = 2.8 \times 10^{-7}$ pc^{-3}. These values are in excellent agreement with those found with the PGS + 20 sample, namely, $z_e = 500$ pc, $D_0 = 2.9 \times 10^{-7}$ pc^{-3} (see Table 7). On the other hand, the procedure of fitting the now truncated $N(z)$ distribution with an exponential model yields $z_e = 700$ pc, $D_0 = 1.5 \times 10^{-7}$ pc^{-3}, while a similar procedure carried out on the PGS + 20 sample yielded $z_e = 500$ pc, $D_0 = 2.5 \times 10^{-7}$ pc^{-3} (see Table 8). Thus, this independent method, which consists in removing from rather than adding to our sample yields exponential scale heights and space densities for the hot subdwarfs which are consistent with those obtained earlier in § 6.1. Furthermore, our analysis based on the imposition of a bright cutoff confirms as well an earlier result: were the scale height *fixed* at 250 pc, the resulting $\langle V'/V'_m \rangle$ value would be an unsatisfactory 0.61, a clear sign that the value chosen for z_e is wrong.

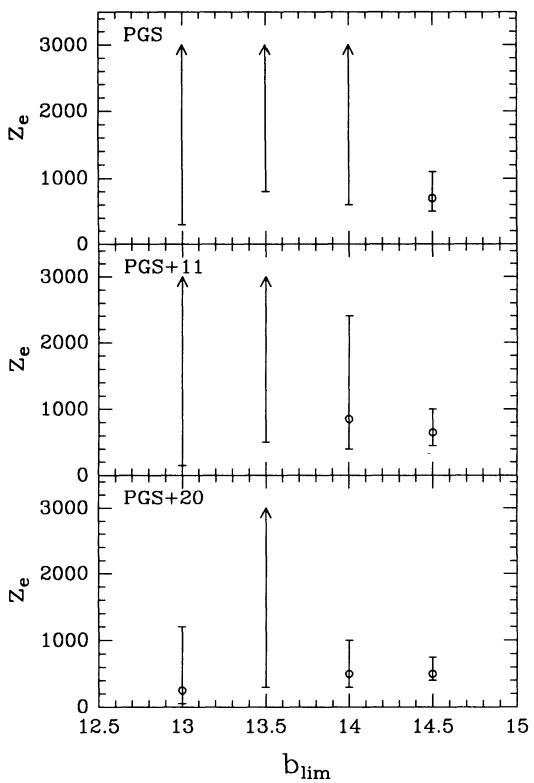

FIG. 10.—Summary of the variation of the characteristic scale height of an exponential distribution as a function of the limiting magnitude, b_{lim}, of the subsample. Temperatures are obtained from Q' or $(u - b)$ (see text), on the basis of the Schulz calibration. This is the so-called GS sequence, where surface gravities are assigned on the basis of $\log g\theta^4 = 2.3$. Arrows indicate that the 90% confidence contour is not closed for $z_e < 4000$ pc, even though lesser-confidence contours might be closed in that window. *Top to bottom:* the PGS subsample, the PGS + 11 subsample, and the PGS + 20 subsample.

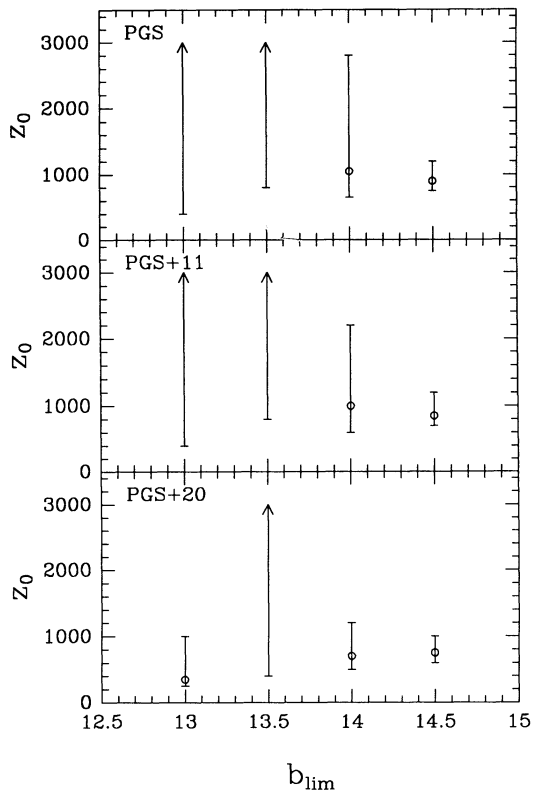

FIG. 11.—Same as Fig. 10, but for an isothermal disk distribution

6.3. *Summary*

The values of the characteristic scale height obtained from our fits to the $N(z)$ distribution within both geometrical models, and for the three samples under consideration (PGS, PGS + 11, and PGS + 20) are summarized in Figures 10 and 11, where they have been plotted as a function of b_{lim}. The arrows indicate lower limits at the 90% confidence level of our fits.

Our results up to now can be further summarized in the following manner: (1) the V/V_m test applied to our various magnitude subsamples suggests that there is a likely dearth of bright objects in the PG survey which may affect the results of statistical analyses of that sample; (2) the space density of hot subdwarfs appears fairly well constrained within an exponential model, and is of the order of $\langle D_0 \rangle = 1.5 \times 10^{-7}$ pc^{-3}, uncertain by a factor of ~ 2; (3) however, it appears difficult to determine with confidence the characteristic scale height of the distribution. Both the traditional V'/V'_m procedure, and direct fits to the $N(z)$ distribution of objects, fail to yield secure and self-consistent estimates of z_e; (4) consideration of an alternative model of the spatial distribution of these objects, an isothermal-disk distribution, yields values of the space density $\langle D_0 \rangle$ similar to those determined earlier. However, problems remain in establishing an unambiguous value for the characteristic scale height of distribution, z_0, within that model; (5) the homogeneity and self-consistency of these results improves significantly when the expected dearth of bright objects in the PG survey is explicitly taken into account. On the basis of statistical samples corrected for missed bright objects or of samples sporting a bright-magnitude cutoff, we derive the following properties for the distribution of hydrogen-rich subdwarfs: a space density of the order of $\langle D_0 \rangle = (3 \pm 1) \times 10^{-7}$ pc^{-3}, and an exponential scale height of the order of $\langle z_e \rangle = 450 \pm 150$ pc or, alternatively, an isothermal disk scale height of the order of $\langle z_0 \rangle = 600 \pm 150$ pc. The latter value is consistent with that determined in the solar neighborhood by van der Kruit & Searle (1981), as well as with the value of z_0 characteristic of the disk of spiral galaxies in general.

7. A COMPARISON WITH PREVIOUS DETERMINATIONS

The results obtained here differ in two significant respects from those of previous analyses (Green et al. 1986; Heber 1986; Downes 1986; Green & Liebert 1987; Moehler et al. 1990a; Bixler et al. 1991; Saffer 1991; Theissen et al. 1993) of the statistical properties of hot, hydrogen-rich subdwarfs: first, our characteristic scale heights of distribution appear consistently larger than the values previously determined, or used, in these investigations. Second, our value of the space density is a factor of 5–10 smaller that those derived earlier.

In general, the space density depends on the statistical sample under consideration, the scale height adopted, and the absolute visual magnitude, M_V, of the objects in the sample. The scale height, in turn, can be either assumed, or derived on the basis of a V'/V'_m test. Most of the differences noted earlier can be traced back to one or several of these steps. Note that, everything else being equal, the use of a larger scale height will yield a smaller space density.

7.1. *Downes (1986)*

Downes (1986), in his Galactic plane survey, derives an exponential scale height z_e of 175 pc, and finds a space density in the range $(1.5–2.0) \times 10^{-6}$ pc^{-3}. His sample of sdB stars contains 31 objects brighter than $B_{pg} = 15.3$, the magnitude cutoff required to satisfy the V'/V'_m test for the KPD white dwarf sample. The scale height z_e is determined by requiring that the V'/V'_m test be satisfied as well with the sample of sdB stars at hand: this procedure imposes $z_e \geq 150$ pc, and Downes adopts $z_e = 175$ pc for the rest of his analysis.

Because the KPD survey is concentrated in the Galactic plane, interstellar extinction is a critical factor in his determination of M_V. Individual distances are derived from a reddening versus distance relationship, and the reddening itself is established from the observed $(B-V)$ and an assumed average $(B-V)_0$ value. The mean M_V for the KPD subdwarfs is 5.0–5.3, depending on the assumed intrinsic color, values 1.3–1.6 mag fainter than the mean of our own reference sample ($\langle M_V \rangle = 3.7$; see Table 1). This difference is sufficient to generate nearly an order of magnitude difference in the space density, since the use of Downes's fainter mean M_V instead of our own leads to individual distances a factor of ~ 2 smaller than those in our original estimate. Thus all the volume elements V'_m, which scale as d^3, are 8 times smaller, and the total space density 8 times larger. Downes's use of a value of z_e generally smaller than the values suggested here also leads to larger space densities, but this is not a particularly important effect in this context, because of the low $\langle z \rangle$ values which characterize the KPD survey.

7.2. *Green et al. (1986) and Green & Liebert (1987)*

In a preliminary analysis based on the then recently completed PG survey, Green et al. (1986) compute the sum of the $1/V'_m$ for all sdB stars of the entire survey using Downes's M_V of 5.0 to determine individual distances. They require an exponential scale height z_e of 325 pc to match Downes's space density in the plane of 1.5×10^{-6} pc^{-3}. Were we to adopt this value of z_e, we would find, for the $b_{lim} = 14.5$ GS sequence, a space density of 5.1×10^{-7} pc^{-3}. This result differs from that of Green et al. by a factor of ~ 3. It turns out, rather coincidentally, that the individual volume elements V'_m should be comparable in the two investigations, because Green et al. use both a fainter absolute magnitude for their stars and a fainter limiting magnitude for their survey (the $B_{pg} \sim 16.2$ limit of the whole PG survey). Because of this, the space density, which involves a sum over the individual V'_m, scales approximately linearly with the number of objects. Green et al. use the whole PG survey, with its 684 objects; we use here 182 objects down to $b_{lim} = 14.5$. The ratio between the sizes of the samples used (~ 3.7) matches approximately the observed ratio of space densities (~ 3).

In a more recent reinvestigation of this problem, Green & Liebert (1987) use an early subset, containing 69 PG objects, of the sample of photoelectric Strömgren observations of Paper I, and *assume* an exponential scale height $z_e = 250$ pc. Note that, as already discussed above and illustrated in Table 3, the V'/V'_m test suggests that this value of z_e does not satisfy the V'/V'_m test for our pared-down subsamples reaching down to $b_{lim} = 14.0$ or $b_{lim} = 14.5$. Their analysis yields a space density of hydrogen-rich subdwarfs of 2.4×10^{-6} pc^{-3}. Had we adopted this exponential scale height in concert with our $b_{lim} = 14.5$ GS sequence, the space density obtained from the $1/V'_m$ summing would be 8.7×10^{-7} pc^{-3} (see Table 3), within a factor of ~ 3 of that of Green & Liebert.

7.3. *Heber (1986) and Moehler et al. (1990a)*

Heber (1986) determines an exponential scale height, z_e, of 190 pc, and derives, with the $1/V'_m$ technique, a space density of 4×10^{-6} pc^{-3} with a sample of 12 sdB taken from the Slettebak & Brundage (1971) objective-prism survey. More recently, Moehler et al. (1990a) determined a new value of z_e, 250 pc, which is consistent with the earlier result, and find, with the same technique, a space density of 1.0×10^{-6} pc^{-3} for a sample of 11 sdB stars taken from the PG survey. The latest determination of Theissen et al. (1993) corroborates these values.

We have already noted in § 3.3 the differences in the derived values of M_V in the three investigations concerned. For the subsamples used for statistical purposes, the mean values are $\langle M_V \rangle = 4.2$ for the 12 objects of Heber (1986); $\langle M_V \rangle = 3.2$, estimated for the statistical sample of 11 objects selected by Moehler et al. (1990a); and $\langle M_V \rangle = 3.70$ for our own reference sequence. Clearly, these differences will impact on the determination of D_0, in the sense seen above that a brighter mean M_V value generally leads to smaller space densities.

As far as the value of z_e is concerned, both Heber (1986) and Moehler et al. (1990a) determine z_e by fitting by exponential distribution to the observed $N(z_i)$ distribution. While this is conceptually similar to one of our own procedures, the method used is quite different. For a small differential field, the number of stars within a bin located at z and of width Δz is given by

$$N(z) = \frac{D_0 \omega z^2 \Delta z}{\sin^3 b} \exp\left(-\frac{z}{z_e}\right), \quad (11)$$

where ω and b are the values appropriate to the small field. Then, for this small field,

$$\ln N - 2 \ln z = -z/z_e + \ln (D_0 \omega \Delta z / \sin^3 b) . \quad (12)$$

A plot of $(\ln N - 2 \ln z)$ versus z thus has a slope of $-1/z_e$. Both Heber and Moehler et al. use plots of $\ln N - 2 \ln z$ to determine z_e.

We make the following two comments on this approach to determine z_e: First, as was shown earlier, for a survey which comprises more than one small field, equation (11) should be summed over all fields, each characterized by its own value of ω_j and b_j, and integrated over z from $z - \Delta z/2$ to $z + \Delta z/2$. However, this summing makes the use of equation (12) somewhat problematic, since the term $\omega/\sin^3 b$ is ill-defined.

Second, and more important, when one attempts to fit a straight line through the $\ln N - 2 \ln z$ values, one invariably finds a mean slope that reduces to the gradient of $-2 \ln z$ between the first and last bin, since the $\ln N$ term is negligible compared to the $-2 \ln z$ term. Neglecting the $\ln N$ term altogether would lead to the following *approximate* form for the slope:

$$-\frac{1}{z_e} \simeq \frac{2 \ln (z_n/z_1)}{z_n - z_1} , \quad (13)$$

where z_1 and z_n are the z-values associated with the first and last bins, respectively. Table 10 presents the scale heights obtained from the formal linear regression of the $(\ln N - 2\ z)$ data carried out by these authors, called there z_{lr}, as well as our approximate value of that quantity, as predicted from equation (13), which we call z_a. The Heber 1986.1 and 1986.2 results represent different fits to the same data set. In the first case, the two stars with the largest values of z are ignored, while in the other case (1986.2), all 10 stars are included up to $z = 1100$ pc. The final value of $z_e = 190$ pc, quoted earlier from Heber (1986), is a mean of these two values. It is clear from these tests that the z_e values generated by the linear regression of these authors can be reproduced satisfactorily by our approximate treatment. To pursue the argument further, we have, in addition, determined z_e for our own data sets with the $\ln N - 2 \ln z$ prescription. These results are also summarized in Table 10. Once again, the linear regression results can be fairly accurately reproduced by simply taking the difference between the first and last bins, as asserted above. It is thus clear, from an examination of equation (13), that the values of z_e generated from a linear regression of that nature are simply related to the depth of the survey, and by no means to the z distribution itself; this method yields values of z_e which increase monotonically as the limiting depth of the sample increases. It is clearly no accident that the value of z_e we derive here on the basis of our own $b_{lim} = 14$ GS sample (235–260 pc) is entirely consistent with that derived by Moehler et al. (1990a), namely, 250 pc, on the basis of their small subsample of PG stars *which reaches down to* $B_{pg} = 14.0$.

TABLE 10

CALCULATED (z_{lr}) VERSUS APPROXIMATED (z_a) VALUES OF EXPONENTIAL SCALE HEIGHT

Sample	z_{lr} (pc)	z_a (pc)	z_h (c)
Heber 1986.1	184	182	900
Heber 1986.2	222	210	1100
Moehler et al. 1990a	250	210	1100
$b_{lim} = 13.0$ GS	176	195	1000
$b_{lim} = 13.5$ GS	230	210	1100
$b_{lim} = 14.0$ GS	260	235	1300
$b_{lim} = 14.5$ GS	285	280	1700
$b_{lim} = 15.0$ GS	305	305	1900

Had we adopted the same exponential scale height ($z_e = 250$ pc), the same subsample of 11 objects, and the same limiting magnitude ($B_{pg} = 14.0$ or $b_{lim} \sim 14.2$) as Moehler et al. (1990a), but our own techniques for assigning distances (or M_V), the $1/V'_m$ method would have yielded a space density of 8.8×10^{-7} pc^{-3} for the Schulz transformation and 9.4×10^{-7} pc^{-3} for the Olson transformation.[7] Both these values are in good agreement with that derived by Moehler et al. (1990a) on the basis of the same sample, namely, 1.0×10^{-6} pc^{-3}. Thus, the differences in the values of D_0 between the work of Moehler et al. (1990a) and our own originate, for the most part, in the different value of z_e derived in these investigations.

7.4. *Bixler et al. (1991)*

This recent statistical analysis is based in part on a high Galactic latitude ultraviolet survey, covering 1300 deg^2, carried out by a balloon-borne telescope. Because of incomplete optical identifications, the sample of 32 sdB stars identified in the colorimetric survey is supplemented by 43 balloon catalog objects identified as sdB stars in the Palomar-Green sample to produce an expanded sample of 75 objects, of which 71 subdwarf stars distributed in 46 fields are ultimately kept. The procedure of Bixler et al. (1991) consists in fitting the observed $N(m_{UV})$ distribution to determine optimal values of the exponential scale height z_e of the distribution, as well as of the space density D_0. Their analysis yields $z_e = 240$ pc, and a corresponding space density of 3.3×10^{-6} pc^{-3}.

There are at least three possible sources for the discrepancy observed between the Bixler et al. results and ours: (1) their $N(m_{UV})$, rather than $N(z)$, fitting procedure; (2) the absolute magnitude adopted for the objects in the sample; and (3) the choice of the statistical sample.

To investigate the first source, we modified our algorithm to apply it to the $N(m_{UV})$ distribution of the Bixler et al. statistical sample. The number $N(m_i)$ of objects observable between the

[7] This comparison can be further extended by using, in addition, the values of M_V derived by Moehler et al. (1990a). In that case, we derive a space density of 9.0×10^{-7} pc^{-3}. The results of the Moehler et al. investigation and ours thus differ by $\sim 10\%$ when similar if not identical input data are used.

ultraviolet magnitudes m_{i-1} and m_{i+1} is thus found by evaluating

$$N(m_i) = \sum_{j=1}^{n} \frac{D_0\,\omega_j}{\sin^3 b_j} \int_{z_{m_{i-1}}}^{z_{m_{i+1}}} z^2 \exp\left(-\frac{z}{z_e}\right) dz\,, \qquad (14)$$

where the integration limits for a given field j are given by

$$z(m_i) = \sin b_j \times 10^{(m_i - A_{UV} - \langle M_{UV}\rangle + 5)/5}\,. \qquad (15)$$

Notice that ω_j represents an effective solid angle, defined for each field as the product of the true solid angle with the fraction of objects in the field that have been identified.

Because of the paucity of the information provided, we cannot reproduce exactly the Bixler et al. analysis but make, instead, the three following assumptions: (1) all 46 fields share a unique Galactic latitude of 60°; (2) the limits of equation (15) are evaluated with $A_{UV} = 0.42$ and $\langle M_{UV}\rangle = 0.73$; and (3) the effective solid angles are adopted as follows: for 22 of the 46 fields, the reported identification rate is an unambiguous 100%; 16 fields have a rate above 50%, which we take here to be 75%; and the last eight have a rate lower than 50%, taken here to be 25%. Under this set of assumptions, our best fit to the resulting $N(m_{UV})$ distribution is obtained for $z_e = 330$ pc and $D_0 = 2.0 \times 10^{-6}$ pc^{-3}, a result consistent with that of Bixler et al. (240 pc; 3.3×10^{-6} pc^{-3}) when the uncertainties about the details of the survey and of the analysis are considered.

The second possible source of difference between the Bixler et al. result and ours is the absolute magnitude used for B subdwarfs. The relevant quantities cannot be compared directly, however, as we use M_b and Bixler et al. use a unique average ultraviolet absolute magnitude, $\langle M_{UV}\rangle$. A first value of $\langle M_V\rangle$ can be derived for the Bixler et al. sample by using the observed y magnitude, their assigned T_{eff} and log g values, as well as our own model atmosphere fluxes (at log $g = 5.0$). Equations (2) and (3) then yield, neglecting the reddening, $\langle M_V\rangle = 4.2$. Again, this comparison is not the whole story, since their adopted average absolute magnitude appears to be independent of the atmospheric parameters they derive for their sources. Perhaps a better way to get at the absolute visual magnitude of the sample is to use their adopted $\langle M_{UV}\rangle = 0.73$ directly to calculate $\langle M_V\rangle$. The models of Wesemael et al. (1980) show that, between 20,000 and 40,000 K, stars at log $g = 5.0$ are, on the average, 3.6 mag fainter at V than at 2000 Å. Thus $\langle M_V\rangle = 4.4$. The Bixler et al. absolute magnitudes, while somewhat fainter than the ones associated with our own analysis (see Table 1), cannot lead to the differences observed between their results and our own.

A third possible consideration, which we find difficult to quantify, is the way the Bixler et al. sample was put together. In retrospect, the idea of combining the optically identified sources with PG objects located in some of the observed fields is not a bad one, since the ultraviolet survey is likely to be more sensitive to the brightest stars which the PG survey tends to miss; the latter, however, becomes rapidly complete at somewhat fainter magnitudes. In fields where the identification rate is 100%, the procedure thus appears to be adequate. But in the 24 other fields where an optical identification of all the sources is not available, the sample most likely remains severely incomplete.

7.5. *Saffer (1991)*

In a recent investigation, Saffer (1991) thoroughly analyzes a sample of 92 stars drawn mostly from the PG survey. These stars are a mix of already identified objects with a wide variety of spectral types (*sd*, *sdB*, *sdB-O*, *sdOA*, *DA*, *BHB*, and *B*), from which he later identifies a subset of 68 confirmed hydrogen-rich subdwarfs. On the basis of an extrapolation of the rate of misidentification found in this sample to the entire PG survey, he deduces the number of objects that are true members of the sdB class.

To proceed to the analysis of the Galactic distribution, Saffer assigns a Galactic height z to each of the selected PG stars, on the basis of the following relationship, obtained from the 68 objects in his sample:

$$\log z = 0.215 B_{pg} - 0.295\,. \qquad (16)$$

Note that this relationship generates an error of the order of 50% in z, since the Galactic latitude in the PG survey varies from 30° to 90°.

Saffer first attempts an analysis of the *differential* $N(z)$ distribution similar to that of Heber and Moehler et al., but he quite sensibly abandons it on the basis of its sensitivity to the choice of bins and misclassification correction (this is not unlike the conclusion reached here in § 7.3). Instead, he opts for fitting the observed *cumulative* $N(z < z_i)$ versus z_i distribution of all the sdB stars down to $B_{pg} = 15.3$ in the PG survey located at a height smaller than z_i. Saffer expresses this quantity in the following manner:

$$N(<z) = C \int_0^z z^2 \exp\left(-\frac{z}{z_e}\right) dz\,. \qquad (17a)$$

The value of the constant C is obtained by normalizing this expression to the observed value $N(z < 985$ pc), the latter being the value of z corresponding to the limiting magnitude of $B_{pg} = 15.3$. Thus,

$$C \equiv N(<z_{lim}) \Big/ \int_0^{z_{lim}} z^2 \exp\left(-\frac{z}{z_e}\right) dz\,. \qquad (17b)$$

His comparison of the observed $f_{cum}(<z) \equiv N(<z)/N(<z_{lim})$ with theoretical curves generated for several values of z_e then yields an optimal exponential scale height of $z_e = 285^{+120}_{-35}$ pc.

With all the fields of the PG survey located above $b = 30°$, the form of equation (17a) breaks down if $z \gtrsim z_{lim} \sin 30° \simeq 493$ pc, and the integrated quantity in that expression then overestimates the true number of stars. This is particularly true for the integral of equation (17b), in which $z_{lim} = 985$ pc, and this will cause the normalization constant C to be underestimated.

In general, the set of equations (17) should be replaced by the following expression:

$$N(<z) = \sum_{j=1}^{n} \frac{D_0\,\omega_j}{\sin^3 b_j} \int_0^{\min[z, z_{max}(j)]} z^2 \exp\left(-\frac{z}{z_e}\right) dz\,, \qquad (18)$$

where $z_{max}(j)$ varies from field to field and depends on the Galactic latitude b_j.

As outlined above, the use of equations (17) instead of equation (18) yields a value of C, related to the midplane density, which is too low. Because of this, the computed values of the normalized integrated numbers of stars (eq. [17a]) are systematically smaller than those observed for all values of z smaller than ~ 500 pc, and a small scale height ($z_e \sim 200$–250 pc), which concentrates the theoretical distribution near the plane of the Galaxy is required to reproduce the observed cumulative distribution at low z. However, for larger values of z, the integral in equation (17a) is overestimated as well, and this tends to

cancel out the underestimate of C; the technique then calls for a more realistic scale height to match the observed cumulative distribution. Figure 5.10 of Saffer (1991), which shows the observed cumulative [$f_{cum}(<z)$] distribution together with a family of theoretical curves associated with different values of z_e, shows precisely the kind of behavior anticipated here: scale heights of the order of 250 pc are suggested for $z \lesssim 600$ pc, while larger values ($z_e \gtrsim 350$ pc) better match the data for $z \gtrsim 600$ pc. Because Saffer's scale-height determination is more heavily weighted toward his results at low z-values, his optimal value of z_e is smaller than that found here, although consistent with it within the respective uncertainties.

8. CONCLUDING REMARKS

Our redetermination of the space density and scale height of hot, hydrogen-rich subdwarfs has significant implications for our understanding of these stars. Our optimal value of D_0, $(3 \pm 1) \times 10^{-7}$ pc^{-3}, essentially independent of the assumed geometrical distribution of stars, is roughly a factor of 5–10 lower than those obtained previously, as summarized in § 1. The resulting birthrate, on the basis of an evolutionary timescale on the extended horizontal branch (EHB) of $\tau \sim 1.5 \times 10^8$ yr, is $\chi_{sdB} \sim (1\text{–}3) \times 10^{-15}$ pc^{-3} yr^{-1}. On the basis of an earlier value of this birthrate based on a statistical analysis of the Slettebak & Brundage (1971) south Galactic pole survey, Heber (1986) had estimated that ~2% of DA white dwarfs originate from (hydrogen-rich) post-EHB stars. In a separate investigation based on a restricted sample isolated by Drilling (1983), Drilling & Schönberner (1985) had suggested that 0.2%–3% of all white dwarfs originated from post-EHB stars, with either a hydrogen-rich or a helium rich atmosphere. A later study (Drilling 1992), based on a slightly expanded sample, permits an improved estimate of ~0.6%. Our new determination—together with the latest value of the white dwarf birthrate given by Weidemann [1990; $\chi_{wd} = (1.5\text{–}2.3) \times 10^{-12}$ pc^{-3} yr^{-1}]—reduces this fraction even more, to ~0.1%. The issue of how this very low rate of input the white dwarf stream can be reconciled with the suggestion of Bergeron et al. (1994) that the low-mass DAO white dwarfs, with their estimated birthrate of $\chi_{DAO} = 2.5 \times 10^{-14}$ pc^{-3} yr^{-1}, are the progeny of post-EHB evolution needs to be carefully looked at.

Equally interesting, in our view, is the fact that the derived scale height of hydrogen-rich subdwarfs appears up to a factor of ~2 larger than those estimated in earlier investigations. The value we determine, within the exponential model, is $z_e = 450 \pm 150$ pc. This result suggests that the hydrogen-rich hot subdwarfs may not represent as homogeneous a population sample as previously thought on the basis of earlier determinations of z_e, which suggested that they belonged to an old disk population (see, e.g., Theissen et al. 1993 for the latest word on this topic). The idea of an admixture of populations is not new; in fact, it can be found in work as early as that of Baschek & Norris (1975), who stated that "while some subdwarf stars are halo objects, a significant proportion of this class belongs to a population having less extreme kinematics." It might, however, be more appropriate today to look at this result within the more refined picture of Galactic structure proposed by Gilmore & Reid (1983), who suggest the presence, in addition to the traditional halo and disk components, of a thick disk, characterized by a scale height $z_e \sim 1350$ pc and accounting for ~2% of the stars in the solar neighborhood. More recent efforts (e.g., von Hippel & Bothun 1993) give $z_e \sim 900$ pc for this new component. While the lower limit to our estimate of z_e (~300 pc) is clearly consistent with a population of old thin-disk stars, our optimal value $z_e \sim 450$ pc is more suggestive of a small admixture of objects characterized by a larger scale height. We note that a similar, albeit more extreme, situation seems to emerge from a detailed analysis of a sample of 21 sdO stars by Thejll et al. (1994), who find their objects to be characterized by rather large distances above the plane ($\langle z \rangle = 0.94$ kpc). On the basis of an earlier, smaller sample, Thejll et al. (1992) had determined a value of the scale height of sdO stars between 460 and 1150 pc. While the similarities between the hydrogen-rich and sdO samples should not be overstated, it remains significant that recent results suggest that the properties of both classes now seem to be in conflict with those of a pure, old disk population group.

We are grateful to the Kitt Peak National Observatory for its long-term support of the observational program which served as the basis for this investigation, and to F. Allard, P. Bergeron, and R. Lamontagne, who all contributed in an essential way to this project. This work was supported in part by the NSERC Canada and by the Fund FCAR (Québec). One of us (B. V.) benefited from the status of Chercheur collégial, granted by the Fund FCAR, while this work was being carried out.

REFERENCES

Allard, F. 1986, M.Sc. thesis, Univ. Montréal
Allard, F., Wesemael, F., Fontaine, G., Bergeron, P., & Lamontagne, R. 1994, AJ, 107, 1565
———. 1995, in preparation
Bahcall, J. N. 1984a, ApJ, 276, 169
———. 1984b, ApJ, 287, 926
Bahcall, J. N., & Soneira, R. M. 1980, ApJS, 44, 73
Barnaby, D., & Thronson, H. A. 1992, AJ, 103, 41
Baschek, B., & Norris, J. 1970, ApJS, 19, 327
———. 1975, ApJ, 199, 694
Baschek, B., Sargent, W. L., & Searle, L. 1972, ApJ, 173, 611
Beers, T. C., Preston, G. W., Shectman, S. A., Doinidis, S. P., & Griffin, K. E. 1992, AJ, 103, 267
Bergeron, P., Fontaine, G., Lacombe, P., Wesemael, F., Crawford, D. L., & Jakobsen, A. M. 1984, AJ, 89, 374
Bergeron, P., Saffer, R. A., & Liebert, J. 1992, ApJ, 394, 228
Bergeron, P., Wesemael, F., Beauchamp, A., Wood, M. A., Lamontagne, R., Fontaine, G., & Liebert, J. 1994, ApJ, 432, 305
Binney, J., & Tremaine, S. 1987, Galactic Dynamics (Princeton: Princeton Univ. Press)
Bixler, J. V., Bowyer, S., & Laget, M. 1991, A&A, 250, 370
Caloi, V. 1989, A&A, 155, 33
Colin, J., et al. 1994, A&A, 287, 38
Downes, R. A. 1986, ApJS, 61, 569
Drilling, J. S. 1983, ApJ, 270, L13
———. 1992, in The Atmospheres of Early-Type Stars, ed. U. Heber & C. S. Jeffery (Berlin: Springer), 257
Drilling, J. S., & Schönberner, D. 1985, A&A, 146, L23
Fleming, T. A., Liebert, J., & Green, R. F. 1986, ApJ, 308, 176
Freeman, K. C. 1970, ApJ, 160, 811
———. 1978, in IAU Symp. 77, Structure and Properties of Nearby Galaxies, ed. E. M. Berkhuijsen & R. Wielebinski (Dordrecht: Reidel), 3
Fuchs, B., & Wielen, R. 1987, in The Galaxy, ed. G. Gilmore & B. Carswell (Dordrecht: Reidel), 375
Gilmore, G., & Reid, N. 1983, MNRAS, 202, 1025
Green, R. F. 1980, ApJ, 238, 685
Green, R. F., & Liebert, J. 1987, in IAU Colloq. 95, The Second Conference on Faint Blue Stars, ed. A. G. D. Philip, J. Liebert, & D. S. Hayes (Schenectady: Davis), 261
Green, R. F., Schmidt, M., & Liebert, J. 1986, ApJS, 61, 305
Greenstein, J. L., & Sargent, A. I. 1974, ApJS, 28, 157
Heber, U. 1986, A&A, 155, 33
———. 1987, in IAU Colloq. 95, The Second Conference on Faint Blue Stars, ed. A. G. D. Philip, J. Liebert, & D. S. Hayes (Schenectady: Davis), 79
———. 1991, in IAU Symp. 145, Evolution of Stars: The Photospheric Abundance Connection, ed. G. Michaud & A. Tutukov (Dordrecht: Kluwer), 363

Heber, U., Hunger, K., Jonas, G., & Kudritzki, R. P. 1984, A&A, 130, 119
Kilkenny, D., Heber, U., & Drilling, J. S. 1988, SAAO Circ. 12
Liebert, J., Saffer, R. A., & Green, E. M. 1994, AJ, 107, 1408
Mihalas, D., & Binney, J. 1981, Galactic Astronomy (San Francisco: Freeman)
Moehler, S., Heber, U., & de Boer, K. S. 1990a, A&A, 239, 265
Moehler, S., Richtler, T., de Boer, K. S., Dettmar, R. J., & Heber, U. 1990b, A&AS, 86, 53
Newell, E. B. 1973, ApJS, 26, 37
Olson, E. C. 1974, PASP, 86, 80
Reid, N., Wegner, G., Wickramasinghe, D. T., & Bessell, M. S. 1988, AJ, 96, 275
Saffer, R. A. 1991, Ph.D. thesis, Univ. Arizona
Saffer, R. A., Bergeron, P., Koester, D., & Liebert, J. 1994, ApJ, 432, 351
Schmidt, M. 1968, ApJ, 151, 393
———. 1975, ApJ, 202, 22
Schulz, H. 1978, A&A, 68, 75
Slettebak, A., & Brundage, R. K. 1971, AJ, 76, 338
Strömgren, B. 1966, ARA&A, 4, 433
Theissen, A., Moehler, S., Heber, U., & de Boer, K. S. 1993, A&A, 273, 524
Thejll, P., Bauer, F., Saffer, R., Kunze, D., Shipman, H., & Liebert, J. 1992, in The Atmospheres of Early-Type Stars, ed. U. Heber & C. S. Jeffery (Berlin: Springer), 261
———. 1994, ApJ, 433, 819
van der Kruit, P. C. 1986, A&A, 157, 230
———. 1988, A&A, 192, 117
van der Kruit, P. C., & Searle, L. 1981, A&A, 95, 105
Villeneuve, B., Wesemael, F., Fontaine, G., Carignan, C., & Green, R. F. 1992, JRASC, 86, 291
von Hippel, T., & Bothun, G. D. 1993, ApJ, 407, 115
Wainscoat, R. J., Freeman, K. C., & Hyland, A. R. 1989, ApJ, 337, 163
Weidemann, V. 1990, in Baryonic Dark Matter, ed. D. Lynden-Bell & G. Gilmore (Dordrecht: Kluwer), 87
Wesemael, F., Auer, L. H., Van Horn, H. M., & Savedoff, M. P. 1980, ApJS, 43, 159
Wesemael, F., Fontaine, G., Bergeron, P., Lamontagne, R., & Green, R. F. 1992, AJ, 104, 203 (Paper I)